Event/Self-Triggered Approximate Leader-Follower Consensus With Resilience to Byzantine Adversaries

Federico M. Zegers, Patryk Deptula, John M. Shea, and Warren E. Dixon, *Fellow, IEEE*

***Abstract*—Distributed event- and self-triggered controllers are developed for approximate leader-follower consensus with robustness to adversarial Byzantine agents for a class of homogeneous multi-agent systems (MASs). A strategy is developed for each agent to detect Byzantine agent behaviors within their neighbor set and then selectively disregard their transmission. Selectively removing Byzantine agents results in time-varying discontinuous changes to the network topology. Nonsmooth dynamics also result from the use of event/self-triggered strategies and triggering condition estimators that enable intermittent communication. Nonsmooth Lyapunov methods are used to prove approximate consensus of the MAS consisting of the remaining cooperative agents. Simulations are included to validate the result and to outline the tradeoff between communication and performance.**

***Index Terms*—Decentralized control, fault tolerant control, multi-agent systems, networked control systems.**

I. Introduction

APPROXIMATE leader-follower consensus along with several other consensus variants have been extensively studied since they have a wide range of applications in multi-agent systems (MASs) and distributed computing (see [1]–[9]). The approximate leader-follower consensus objective is to position the follower agents of an MAS so they converge into a forward-invariant neighborhood of the leader's position. Most consensus results consider continuous-time dynamical MASs and assume continuous communication and sensing. However, physical constraints on a network, like communication bandwidth, data packet losses, and delays, may inhibit continuous communication.

Motivated by intermittent communication challenges, event-triggered control (ETC) enables the manipulation of continuous-time dynamical systems under intermittent state feedback (see [10]–[15]). ETC opportunistically selects when to update the system to efficiently perform a task [16]. With respect to an MAS, interagent communication occurs at times dictated by an event-trigger, which is derived from the need to preserve system stability, and if desired, a performance criterion [17]. For example, the authors in [10] investigate event-triggered pinning control for the synchronization of complex networks of nonlinear dynamical systems. A multi-agent formation control problem is investigated in [18] with ETC updates and additive disturbances, where agents only communicate by exchanging information via a cloud repository. In [12], a decentralized controller is developed that uses ETC scheduling to enable leader-follower consensus under fixed and switching communication topologies.

The event-trigger design can have significant ramifications on the overall system performance. Typically, agents are required to continuously monitor their trigger condition while each neighbor continuously monitors a neighbor's communication. Self-triggered control (STC) provides a more efficient triggering method that leverages the system model to predict when to monitor/communicate (see [19], [20]). Moreover, an STC strategy can also be developed that eliminates the need for an agent's neighbors to continuously monitor for information requests.[1] While ETC and STC strategies provide numerous benefits, critical communication timing conditions introduce potential vulnerabilities. Specifically, since the trigger conditions are based on feedback from multiple agents, erroneous feedback can lead to undesired outcomes.

Assuming knowledge of the number of adversarial agents, the authors in [22] study event-triggered secure cooperative control of linear MASs under denial of service (DoS) attacks, which are

Manuscript received October 7, 2020; accepted March 23, 2021. Date of publication April 21, 2021; date of current version February 28, 2022. This work was supported in part by A Task Order Contract with the Air Force Research Laboratory, Munitions Directorate at Eglin AFB, in part by the Office of Naval Research under Grant N00014-13-1-0151, in part by the NEEC Award N00174-18-1-0003, in part by the AFOSR Award FA9550-18-1-0109, and in part by the AFOSR Award FA9550-19-1-0169. Recommended by Associate Editor R. M. Jungers. *(Corresponding author: Federico Zegers.)*

Federico M. Zegers and Patryk Deptula are with the Department of Mechanical and Aerospace Engineering, University of Florida, Gainesville, FL 32611-6250 USA (e-mail: fredzeg@ufl.edu; pdeptula@ufl.edu).

John M. Shea is with the Department of Electrical and Computer Engineering, University of Florida, Gainesville, FL 32611-6250 USA (e-mail: jshea@ece.ufl.edu).

Warren E. Dixon is with the Department of Mechanical and Aerospace Engineering, University of Florida, Gainesville, FL 32611-6250 USA, and also with the Department of Electrical and Computer Engineering, University of Florida, Gainesville, FL 32611-6250 USA (e-mail: wdixon@ufl.edu).

Color versions of one or more figures in this article are available at https://doi.org/10.1109/TAC.2021.3074849.

Digital Object Identifier 10.1109/TAC.2021.3074849

[1]Eliminating the need for continuous monitoring allows the potential for power savings [21].

defined as interruptions of communication on the control channels carried out by an intelligent adversary. Static networks with cooperative and malicious nodes have been extensively studied within the computer science literature [23], [24], resulting in iterative consensus algorithms for distributed computing applications that are robust to components subject to faults. Different research communities are beginning to extend these architectures to MAS applications consisting of mobile agents, which requires the nontrivial study of motion planning to preserve algebraic graph properties such as connectivity. For example, the authors in [25] address the problem of resilient in-network consensus in the presence of Byzantine nodes [23], where resilience is designed for worst-case security breaches and omnipotent malicious nodes. The weighted-mean-subsequence-reduced (W-MSR) algorithm enables each node to receive state information from its neighbors, sort the states, and neglect at most F extreme states relative to the node's state. While asymptotic consensus is obtained using the W-MSR algorithm, the result requires an upper bound of the maximum number of Byzantine agents. Such an approach requires at least $2F+1$ reliable neighbors, which is difficult to scale with increasing node number. Moreover, information is shared with all agents regardless of their cooperative/Byzantine status, which can impact secure MAS consensus. The result in [26] also enables resilient consensus assuming the maximum number of malicious agents is known. The result in [27] achieves resilient approximate consensus by removing extreme values similar to the W-MSR algorithm while enabling asynchronous communication through a self-triggered strategy given a known upper bound for the maximum number of Byzantine agents. The result in [28] achieves consensus tracking of an arbitrary piecewise continuous step function for a network of agents using the W-MSR algorithm provided the network is strongly $(2F+1)-$robust. While malicious agent identification is not required, MAS consensus is limited to at most F malicious agents. Nonetheless, ETC and STC strategies that enable secure MAS consensus while detecting and mitigating against Byzantine adversaries require further investigation.

In graph theoretic terms, antagonistic interactions can be modeled by replacing the standard communication graph, characterized by nonnegative weights, with a signed graph displaying both positive and negative weights (see [29], [30]). Positive directed/undirected paths correspond to cooperative interactions with agents, while negative directed/undirected paths describe interactions with antagonistic agents. The work in [31] develops the concept of bipartite consensus among agents with antagonistic interaction, where bipartite consensus or agreed dissensus is defined as when all agents in the MAS converge to a state that is the same in magnitude but not in sign, effectively enabling each team to reach their own consensus state. By addressing the classical example of homogeneous agents modeled as simple scalar integrators, the authors in [31] prove that if the signed, weighted, and connected communication graph describing the agents' interactions is structurally balanced, then the agents reach bipartite consensus. If the interactions are antagonistic, but not structurally balanced, the only agreement that can be achieved among the agents is the trivial one, where all the agents' states converge to zero.

The authors in [32] extend the results in [31] to an MAS consisting of N agents with linear time-invariant (LTI) dynamics and establish conditions to ensure consensus and bipartite consensus under the assumption that the agent interactions can be described by a weighted, signed, connected, and structurally balanced graph. Moreover, bipartite consensus can always be reached under the assumption that the agent dynamics are stabilizable. However, consensus to a common state for the two antagonistic groups can be achieved only under more restrictive requirements on the Laplacian associated with the communication graph and on the agents' description. In particular, consensus may be achieved only if there is some equilibrium between the two groups, both in terms of cardinality and in terms of the weights of the conflicting interactions among agents. The result in [33] considers the bipartite consensus problem for an MAS composed of agents with LTI dynamics and input saturation over directed and unbalanced networks.

The works in [31]–[33] share the common goal of enabling both teams in the antagonistic network to reach their own respective consensus, which assumes both consensus states can coexist. However, signed graphs can also be extended to applications, where the goal of one team is to reach consensus while the goal of the opposition is to prevent the other team from reaching consensus. Such a scenario works under the assumption that each team has a goal and must cooperatively work together to reach their goal. However, it is not possible for both teams to reach their goal simultaneously. Hence, if one team is to conspire against the other in a cooperative manner, then signed graphs can be leveraged to model these interactions. However, if one group is organized while the other is not, a traditional graph is sufficient to model the cooperative interactions of the organized team.

In this article, the approximate leader-follower consensus problem for cooperative agents in the presence of Byzantine adversaries is investigated, where approximate leader-follower consensus is achieved when the state of the followers is driven into a forward invariant neighborhood of the state of the leader. Since only the cooperative followers must collaborate to reach leader-follower consensus and the Byzantine adversaries are assumed to operate independently (i.e., do not work together against the cooperative followers), a traditional unsigned graph is used to model the network topology of the followers. Moreover, this article presents event- and self-triggered strategies for the approximate leader-follower consensus problem while providing robustness to Byzantine adversaries. Unlike methods such as W-MSR, that need to know an upper bound on the number of Byzantine agents *a priori* and then reject some amount of outlier information, the work in this article uses a Lyapunov-based detection strategy to identify Byzantine actors online. Motivated by the potential for different ways in which an agent can be compromised (e.g., different combinations of sensing, actuation, or computation) and different potential responses to such behavior as described in Section V-C, we segregate Byzantine agents into different categories. Based on the agent category, the resulting graph can become directed, time-varying, and unbalanced. Despite these complications, the result achieves approximate leader-follower consensus, between the leader and cooperative followers, in a distributed manner, where each agent's control input is computed from local neighbor interactions. Moreover, in the absence of Byzantine adversaries, this work can recover the result in and is a generalization of [12], which did not consider Byzantine agents. The stability of the event- and self-triggered control strategies are examined through a nonsmooth Lyapunov analysis. This work is a generalization of our precursory result in [34]. Specifically, this article provides broader context, additional mathematical development for the stability analysis, a more detailed fault detection method, and simulation results investigating the tradeoff between the event- and self-triggered strategies with respect to power savings, communication bandwidth, and performance.

II. Preliminaries

A. Notation

Let $\mathbb{R}$ and $\mathbb{Z}$ denote the set of real numbers and integers, respectively, where $\mathbb{R}_{\geq 0} \triangleq [0, \infty)$, $\mathbb{R}_{>0} \triangleq (0, \infty)$, $\mathbb{Z}_{\geq 0} \triangleq \mathbb{R}_{\geq 0} \cap \mathbb{Z}$, and $\mathbb{Z}_{>0} \triangleq \mathbb{R}_{>0} \cap \mathbb{Z}$. Let $A \in \mathbb{R}^{p \times q}$ be a real-valued $p \times q$ matrix, where $p, q \in \mathbb{Z}_{>0}$. If $p = q$ and A has real eigenvalues, then the maximum and minimum eigenvalues of A are denoted by $\lambda_{\max}(A) \in \mathbb{R}$ and $\lambda_{\min}(A) \in \mathbb{R}$, respectively. If $p \neq q$, then the maximum singular value of A is denoted by $S_{\max}(A) \in \mathbb{R}_{\geq 0}$. The $p \times q$ zero matrix and the $p \times 1$ zero vector are denoted by $0_{p \times q}$ and 0_p, respectively. Let $1_p \in \mathbb{R}^p$ denote a column vector with all entries being 1. The $p \times p$ identity matrix is denoted by I_p. The Euclidean norm of a vector $r \in \mathbb{R}^p$ is denoted by $\|r\| \triangleq \sqrt{r^T r}$. The Kronecker product of $A \in \mathbb{R}^{p \times q}$ and $B \in \mathbb{R}^{u \times v}$ is denoted by $(A \otimes B) \in \mathbb{R}^{pu \times qv}$. The symbols $\wedge$, $\vee$, and $\neg$ denote logical AND, OR, and NOT, respectively. Let $2^{\mathcal{S}}$ denote the power set of the set $\mathcal{S}$.

B. Algebraic Graph Properties

Let $\mathcal{G}(t) \triangleq (\mathcal{V}, \mathcal{E}(t), \mathcal{A}(t))$ be a time-varying, weighted, and undirected graph with node set $\mathcal{V} \triangleq \{1, 2, \ldots, N\}$ for some $N \in \mathbb{Z}_{>0}$, undirected edge mapping $\mathcal{E} : [0, \infty) \to 2^{\mathcal{V} \times \mathcal{V}}$, and weighted adjacency mapping $\mathcal{A} : [0, \infty) \to \mathbb{R}_{\geq 0}^{N \times N}$, where $\mathcal{A}(t) \triangleq [a_{ij}(t)]$ and $a_{ij} : [0, \infty) \to \{0, 1\}$. Note that $a_{ij}(t) = 1$ implies node i can receive information from node j, and $a_{ij}(t) = 0$ implies node i cannot receive information from node j, where only binary weights are considered. Within the context of this article, no self-loops are considered, and therefore, $a_{ii}(t) \triangleq 0$ for all $i \in \mathcal{V}$ and $t \geq 0$. In general, $a_{ij}(t) \neq a_{ji}(t)$, but equality is possible. An undirected edge is defined as an ordered pair (j, i), where $(j, i) \in \mathcal{E}(t)$ if and only if $(i, j) \in \mathcal{E}(t)$. Note that $(j, i) \in \mathcal{E}(t)$ implies node j can send information to node i. An undirected path is a sequence of edges in $\mathcal{E}(t)$. An undirected graph is called connected if and only if there exists an undirected path between any two distinct nodes. The time-varying neighbor set of node i is defined by $\mathcal{N}_i : [0, \infty) \to 2^{\mathcal{V}}$, where $\mathcal{N}_i(t) \triangleq \{j \in \mathcal{V} : (j, i) \in \mathcal{E}(t), j \neq i\}$.

The diagonal degree mapping $\Delta : [0, \infty) \to \mathbb{R}_{\geq 0}^{N \times N}$ of the undirected graph $\mathcal{G}(t)$ is defined by $\Delta(t) \triangleq [\Delta_{ij}(t)]$, where for all $i \neq j$ and $t \geq 0$, $\Delta_{ij}(t) \triangleq 0$ and $\Delta_{ii}(t) \triangleq \sum_{j \in \mathcal{V}} a_{ij}(t)$. The graph Laplacian $L : [0, \infty) \to \mathbb{R}^{N \times N}$ of the undirected graph $\mathcal{G}(t)$ is defined by $L(t) \triangleq \Delta(t) - \mathcal{A}(t)$. Consider a single node, indexed by 0, along with the mapping $D : [0, \infty) \to \mathbb{R}_{\geq 0}^{N \times N}$, such that $D \triangleq [d_{ij}]$ and $d_{ij} : [0, \infty) \to \{0, 1\}$. For all $i \neq j$ and $t \geq 0$, $d_{ij}(t) \triangleq 0$. Let $d_i(t) \triangleq d_{ii}(t)$, where $d_i(t) = 1$ if node 0 can send information to node i, and $d_i(t) = 0$ otherwise. Hence, the weighted connectivity matrix encoding all communication links between all nodes in $\mathcal{V} \cup \{0\}$ is given by the mapping $H : [0, \infty) \to \mathbb{R}^{N \times N}$, where $H(t) \triangleq L(t) + D(t)$.

Remark 1: While $H(t)$ is a time-varying matrix, the set $\{H(t)\}$ is finite since there are a finite number of configurations in which the agents of the MAS can be connected.

III. Agent Dynamics and Network Topology

Consider a homogeneous MAS consisting of a single leader indexed by 0 and a set of $N \in \mathbb{Z}_{>0}$ follower agents indexed by $\mathcal{V}$. The linear time-invariant model of agent $i \in \mathcal{V} \cup \{0\}$ is

$$\dot{x}_i(t) = Ax_i(t) + Bu_i(t), \quad (1)$$

where $x_i : [0, \infty) \to \mathbb{R}^m$ denotes the position, $\dot{x}_i : [0, \infty) \to \mathbb{R}^m$ denotes the velocity, $A \in \mathbb{R}^{m \times m}$ denotes the known constant state matrix, $B \in \mathbb{R}^{m \times n}$ denotes the known full-row rank control effectiveness matrix, and $u_i : [0, \infty) \to \mathbb{R}^n$ denotes the control input for agent i. Within this article, the followers can be categorized as either Byzantine or cooperative. Let the mapping $\mathcal{B} : [0, \infty) \to 2^{\mathcal{V}}$ define the time-varying set of Byzantine agents and the mapping $\mathcal{C} : [0, \infty) \to 2^{\mathcal{V}}$ define the time-varying set of cooperative agents, where $\mathcal{B}(t) \cap \mathcal{C}(t) = \varnothing$ and $\mathcal{B}(t) \cup \mathcal{C}(t) = \mathcal{V}$ for all $t \geq 0$. The following assumptions are made to facilitate the subsequent analysis.

Assumption 1: Each agent is capable of measuring its own position for all $t \geq 0$.

Assumption 2: The pair (A, B) is stabilizable.

Assumption 3: The control and state of the leader are continuous and bounded, i.e., there exists $M_0, \overline{M}_0 \in \mathbb{R}_{>0}$, such that $\|u_0(t)\| \leq M_0$ and $\|x_0(t)\| \leq \overline{M}_0$ for all $t \geq 0$.

The flow of information between the followers of the MAS is modeled by a time-varying, weighted, and undirected graph $\mathcal{G}(t) = (\mathcal{V}, \mathcal{E}(t), \mathcal{A}(t))$. Within this article, $(j, i) \in \mathcal{E}(t)$ if and only if $\|x_i(t) - x_j(t)\| \leq R_{\text{com}}$, where $R_{\text{com}} \in \mathbb{R}_{>0}$ denotes the communication radius of each agent $i \in \mathcal{V} \cup \{0\}$. It then follows that $\mathcal{N}_i(t) = \{j \in \mathcal{V} \setminus \{i\} : \|x_i(t) - x_j(t)\| \leq R_{\text{com}}\}$. Let $\mathcal{E}_C(t)$ denote the undirected edge set and $\mathcal{A}_C(t)$ denote the weighted adjacency matrix associated with all cooperative followers in $\mathcal{C}(t)$. The sub-MAS consisting of only the cooperative followers is modeled by the time-varying, weighted, and undirected graph $\mathcal{G}_C(t) \triangleq (\mathcal{C}(t), \mathcal{E}_C(t), \mathcal{A}_C(t))$ and is referred to as the cooperative MAS (CMAS).

Assumption 4: The leader is a cooperative agent for all $t \geq 0$.

Assumption 5: The graph $\mathcal{G}_C(t)$ is connected for all $t \geq 0$, and $d_i(t) = 1$ for some $i \in \mathcal{C}(t)$ for all $t \geq 0$.[2]

IV. Objectives

The objective is to design distributed event- and self-triggered controllers for each cooperative agent governed by (1) to

[2]Future works will develop network connectivity maintenance methods for the CMAS. Potential inroads to such results include [35].

achieve approximate leader-follower consensus while identifying Byzantine adversaries and disregarding their disruptive inputs. Resilience to Byzantine adversaries is achieved by providing each follower the ability to detect Byzantine agents in their neighbor set and delete existing edges between themselves and all Byzantine neighbors. The result ensures each cooperative agent coordinates its motion based only on information from cooperative neighbors yielding $\mathcal{G}_C(t)$. To quantify the consensus objective, let $e_{1,i} : [0, \infty) \rightarrow \mathbb{R}^m$ be defined as

$$e_{1,i}(t) \triangleq x_i(t) - x_0(t). \tag{2}$$

Approximate leader-follower consensus is achieved when $e_{1,i}(t)$ is uniformly ultimately bounded (UUB) for all cooperative followers $i \in \mathcal{V}$. Since the behavior of Byzantine agents cannot be guaranteed, the objective can only be satisfied by the cooperative agents. The use of ETC/STC methods also motivates the development of an observer to provide state estimates. The state estimation error of follower i is defined by $e_{2,i} : [0, \infty) \rightarrow \mathbb{R}^m$, where

$$e_{2,i}(t) \triangleq \hat{x}_i(t) - x_i(t) \tag{3}$$

such that $\hat{x}_i : [0, \infty) \rightarrow \mathbb{R}^m$ denotes the state estimate of x_i for each $i \in \mathcal{V}$.

In Section V, the Byzantine adversary model, detection strategy, and mitigation protocol are presented. A general detection method enables each follower to distinguish between cooperative and Byzantine neighbors, and one such approach is introduced in Section V-B. Section V-C then presents a method enabling each follower to disregard data transmissions from Byzantine neighbors to satisfy the objective. In Section VI-A, an event-triggered strategy that satisfies the objective is developed, where Section VI-B provides a stability analysis for the controller and observer presented in Section VI-A. Section VI-C completes the ETC development by excluding the possibility of Zeno behavior for the proposed event-trigger. Section VII provides an STC extension, and Section VIII illustrates and compares the performance of the ETC and STC methods.

V. Agent Models, Detection, and Mitigation

A detection method is presented in this section that provides distributed detection, where each agent formulates an inequality-based test to determine if an agent is Byzantine. Since (sufficiently disturbing) Byzantine actions violate the inequality, the detection method is considered instantaneous (or finite-time over the duration between communication events) in the sense that the inequality condition is interrogated at each communication event. Example strategies that enable finite-time Byzantine agent detection include [36]–[39]. Note that the methods in [36]–[38] are not directly applicable to the results in this article since these techniques utilize observers that require continuous communication. Furthermore, while [39] provides an alternative detection strategy, like our detector, it also does not guarantee detection of Byzantine adversaries that have complete knowledge of the detection strategy.

A. Agent Definitions

In this article, a Byzantine agent is defined as a noncompliant follower (cf. [23], [40]). Since noncompliance covers a broad scope of behaviors, we narrow our focus to two types of Byzantine agents, namely, Type I and Type II. A Type I Byzantine agent is defined as a follower that executes the intended controller but communicates false state information about itself to its neighbors. A Type II Byzantine agent is defined as a follower that executes a controller that is different from the intended controller or executes the intended controller under the influence of faulty hardware, while communicating true or no state information about itself to its neighbors. Consequently, a Type I Byzantine agent remains within the communication range of the CMAS since a Type I Byzantine agent executes the intended controller. In contrast, a Type II Byzantine agent may potentially leave the communication range of the CMAS. Note that nonresponsive communication is a characteristic of Type II Byzantine behavior and can occur due to a follower leaving the CMAS, radio failure, or malicious intent. A cooperative agent is defined as a follower that successfully executes the intended controller and provides true state information about itself to all its neighbors.

B. Agent Models and Detection

The Byzantine agent detection problem is similar to fault detection since a Byzantine agent can elicit undesirable behavior in an MAS. Several methods can enable Byzantine agent detection, e.g., performance-based fault detection and model-based fault detection [41], [42]. Such detection strategies are threshold-based methods, which compare an error metric to some user-defined threshold. There are multiple ways to determine a threshold, e.g., through a statistical analysis of data generated by a simulation/experimental study or an analysis-based derivation. Yet, no threshold strategy is perfect, and we cannot guarantee Byzantine agent detection for all instances and all types of Byzantine behavior. Hence, Byzantine agent detection is an open problem that requires further investigation.

Let $\{t_k^i\}_{k=0}^{\infty} \subset \mathbb{R}_{\geq 0}$ be an increasing sequence of event-times determined by a subsequently defined event-trigger (see Theorem 1). Note that t_k^i denotes the k^{th} instance follower i broadcasts its state to its neighbors. Suppose follower i broadcasts its state information to all followers $j \in \mathcal{N}_i(t)$ at time t_k^i, where $x_i(t_k^i)$ denotes the true state of follower i at time t_k^i, and $x_{i,j}(t_k^i) \in \mathbb{R}^m$ denotes the state information that is broadcast from follower i to follower j at time t_k^i. Given the ETC strategy, the state estimate of follower i is reset to the broadcast state of follower i as defined in (11), where $\hat{x}_i(t_k^i) = x_{i,j}(t_k^i)$ for each $j \in \mathcal{N}_i(t)$. Moreover, let $\hat{x}_i^-(t_k^i)$ denote the state estimate of follower i the moment before being reset to $x_{i,j}(t_k^i)$, where the mismatch between the state estimate of follower i before and after the reset at time t_k^i with respect to follower j is defined as

$$\bar{e}_{i,j}\left(t_k^i\right) \triangleq \hat{x}_i^-\left(t_k^i\right) - x_{i,j}\left(t_k^i\right). \tag{4}$$

Similarly, let

$$e_{2,i}^-\left(t_k^i\right) \triangleq \hat{x}_i^-\left(t_k^i\right) - x_i^-\left(t_k^i\right) \tag{5}$$

denote the state estimation error of follower i the moment before being reset at time t_k^i. In a cooperative setting, follower i broadcasts its true state to all of its neighbors at time t_k^i, i.e., $x_i(t_k^i) = x_{i,j}(t_k^i)$ for all $j \in \mathcal{N}_i(t)$, where it can be shown that $e_{2,i}^-(t_k^i) = \bar{e}_{i,j}(t_k^i)$. Let $\Psi_{i,k}$ denote an upper bound[3] for $\|e_{2,i}^-(t_k^i)\|$, where

$$\left\|e_{2,i}^-\left(t_k^i\right)\right\| \leq \Psi_{i,k}. \tag{6}$$

Since $\|e_{2,i}^-(t_k^i)\| = \|\bar{e}_{i,j}(t_k^i)\|$ and $\|e_{2,i}^-(t_k^i)\| \leq \Psi_{i,k}$, $\|\bar{e}_{i,j}(t_k^i)\| \leq \Psi_{i,k}$. However, within a contested environment, it is possible for $x_i(t_k^i)$ to differ from $x_{i,j}(t_k^i)$, i.e., follower i can provide misinformation about its state. Therefore, the Byzantine agent detector that follower j uses to determine the status of follower $i \in \mathcal{N}_j(t)$ at time t_k^i is[4]

$$\Xi_{i,k} \triangleq \left\|\bar{e}_{i,j}\left(t_k^i\right)\right\| - \Psi_{i,k}, \tag{7}$$

where follower i is a cooperative neighbor of follower j at time t_k^i if $\Xi_{i,k} \leq 0$, and follower i is a Byzantine neighbor of follower j at time t_k^i if $\Xi_{i,k} > 0$. The estimated state of follower i before the reset is compared to the potential state estimate update of follower i after the reset in (4). Therefore, this strategy enables instantaneous detection of Byzantine adversaries that provide sufficiently disturbing state information.

The following atomic propositions are presented to precisely model the behavior of Type I Byzantine agents, Type II Byzantine agents, and cooperative agents within this article. Let $\mathcal{D}_{k,i}$ define the statement $\Xi_{i,k} \leq 0$, $\mathcal{X}_{i,j}$ define the statement $x_i(t) = x_{i,j}(t)$, and $\mathcal{T}_{k,i}$ define the statement $t_k^i \leq t_{k-1}^i + \Delta_i$, where $\Delta_i \in \mathbb{R}_{>0}$ is a constant parameter that is defined in Remark 6. Hence, $\mathcal{D}_{k,i}$, $\mathcal{X}_{i,j}$, and $\mathcal{T}_{k,i}$ are each either true or false.

Observe that $\mathcal{D}_{k,i}$, $\mathcal{X}_{i,j}$, and $\mathcal{T}_{k,i}$ encode acceptable agent motion, honest state reporting, and punctual state reporting, respectively, for follower i at time t_k^i. With respect to follower j and for each broadcast time t_k^i, follower $i \in \mathcal{N}_j(t)$ is

$$\begin{cases} \text{cooperative}, & \mathcal{D}_{k,i} \wedge \mathcal{X}_{i,j} \wedge \mathcal{T}_{k,i} \\ \text{Type I}, & \neg\left(\mathcal{D}_{k,i} \vee \mathcal{X}_{i,j}\right) \wedge \mathcal{T}_{k,i} \\ \text{Type II}, & \neg\left(\mathcal{D}_{k,i} \wedge \mathcal{T}_{k,i}\right) \wedge \mathcal{X}_{i,j}. \end{cases} \tag{8}$$

Hence, given the agent models in (8), the set of cooperative neighbors of follower j is given by

$$\mathcal{C}_j(t) \triangleq \left\{i \in \mathcal{N}_j(t) : \forall t_k^i \leq t \; \mathcal{D}_{k,i} \wedge \mathcal{T}_{k,i}\right\},$$

and the set of Byzantine neighbors of follower j is given by

$$\mathcal{B}_j(t) \triangleq \left\{i \in \mathcal{N}_j(t) : \exists t_k^i \leq t \; \neg\left(\mathcal{D}_{k,i} \wedge \mathcal{T}_{k,i}\right)\right\}.$$

By convention, if follower i does not provide follower j with state information within a predetermined time period, i.e., $t_k^i > t_{k-1}^i + \Delta_i$, then follower j categorizes follower i as Byzantine, i.e., $i \in \mathcal{B}_j(t)$. Efforts in this article focus only on detectable Type I and Type II behaviors, and additional efforts are required to generalize the development to broader classes of adversarial behaviors.

[3]See Remark 5 (for ETC) or Remark 8 (for STC) for specific examples of $\Psi_{i,k}$.

[4]$\Psi_{i,k}$ in (6) represents a threshold that is used for Byzantine agent detection. As with any threshold detection method, if the adversary knows this threshold, then it can inject small perturbations below the threshold to yield some effect. These small perturbations can be modeled as a bounded disturbance, which leads to a larger UUB bound given the proposed controller. An open problem for all such detection strategies is to determine the most sensitive threshold that balances detection with false positives, especially in the presence of noise.

C. Mitigation

Since the objective is to achieve approximate leader-follower consensus by the cooperative followers, and both the detector in (7) and the communication timing condition, i.e., $t_k^i \leq t_{k-1}^i + \Delta_i$, allows each follower to identify their cooperative and Byzantine neighbors, the edge weights can be intermittently updated according to the status of each neighbor. Hence, for all $t \in [t_k^j, t_{k+1}^j)$, the piecewise constant edge weight $a_{ij}(t)$ is defined by

$$a_{ij}(t) \triangleq \begin{cases} 1, & j \in \mathcal{C}_i(t) \\ 0, & j \in \mathcal{B}_i(t). \end{cases} \tag{9}$$

From (9), the edge weight $a_{ij}(t) = 1$ for all $t \in [t_k^j, t_{k+1}^j)$ if follower j is a cooperative neighbor of follower i at time t_k^j, and $a_{ij}(t) = 0$ for all $t \in [t_k^j, t_{k+1}^j)$ if follower j is a Byzantine neighbor of follower i at time t_k^j.

Although the proposed detection and mitigation strategy enables each cooperative agent to insulate itself from Byzantine neighbors, the choice remains to allow each cooperative agent to communicate state information about itself to Byzantine neighbors or not. Communication could enable a Type I Byzantine adversary to be regulated to a desired location for remediation. However, communicating with a compromised agent could endanger security. Without loss of generality, the subsequent work enables communication from cooperative agents to their Byzantine neighbors.

Assumption 6: For all $j \in \mathcal{B}_i(t)$ and each $i \in \mathcal{V}$, follower i communicates state information about itself to follower j.[5]

Remark 2: While a threshold-based detection strategy is used to categorize the neighbors of follower i as either cooperative or Byzantine for each $i \in \mathcal{V}$, any other detection method that enables the construction of (9) can be implemented along with the observer in (10)–(11), controller in (12)–(13), and event-trigger in (24) to achieve the objective.

VI. State Estimation and Event-Triggered Control

A. Control and Observer Development

Given the use of an event-triggered strategy, the state estimate of follower $j \in \mathcal{V}$ is generated by the following observer:

$$\dot{\hat{x}}_j(t) \triangleq A\hat{x}_j(t), \; t \in \left[t_k^j, t_{k+1}^j\right) \tag{10}$$

$$\hat{x}_j\left(t_k^j\right) \triangleq x_{j,i}\left(t_k^j\right), \tag{11}$$

which is synchronized among all followers $i \in \mathcal{N}_j(t) \cup \{j\}$. Note that for each $j \in \mathcal{V}$, self-communication does not occur and $\hat{x}_j(t_k^j) \triangleq x_j(t_k^j)$. Moreover, recall that $x_{j,i}(t_k^j) = x_j(t_k^j)$ provided follower j is cooperative. The solution to (10) over $[t_k^j, t_{k+1}^j)$ is $\hat{x}_j(t) = e^{A(t-t_k^j)}\hat{x}_j(t_k^j)$. Hence, accurate estimation

[5]The leader will also communicate state information about itself to its neighbors.

of the state of follower j requires an accurate initial condition, i.e., correct state estimation is ensured provided $\hat{x}_j(t_k^j) = x_j(t_k^j)$. Therefore, in this article, if $j \in \mathcal{B}_i(t_k^j)$, then $j \in \mathcal{B}_i(t)$ for all $t \geq t_k^j$. The Byzantine designation is permanent since follower i does not have an accurate state of the follower in question with which to propagate the estimate forward and compare to the corresponding sampled state. There are various methods to allow the inclusion of a rehabilitated follower into the cooperative follower set, e.g., trusted third party information can be used to reset the observer or a reputation algorithm such as in [43] can potentially be used as an alternative to adjust the graph edge weights. These potential extensions merit further investigation and are beyond the scope of this article.

Assumption 7: All followers are cooperative agents at time $t = 0$.

Assumption 7 enables the detection of Byzantine followers after the initial time $t = 0$. Like most fault or change detection methods, a baseline condition (i.e., at $t = 0$) is first required for comparison (cf. [41], [42]). However, Byzantine follower detection can be accomplished using the threshold-based detector in (7) at the initial time provided all followers know the initial position of their neighbors. Motivated by [12], the controller for follower $i \in \mathcal{V}$ is

$$u_i(t) \triangleq K z_i(t) + K e_{2,i}(t) \tag{12}$$

$$z_i(t) \triangleq \sum_{j \in \mathcal{N}_i(t)} a_{ij}(t) \left(\hat{x}_j(t) - \hat{x}_i(t)\right) + d_i(t) \left(x_0(t) - \hat{x}_i(t)\right), \tag{13}$$

where $z_i : [0, \infty) \to \mathbb{R}^m$ is the estimate-based consensus control effort. The gain matrix $K \in \mathbb{R}^{n \times m}$ in (12) is designed as $K \triangleq B^T P$, where $P \in \mathbb{R}^{m \times m}$ is the symmetric and positive definite solution to the algebraic Riccati equation (ARE) given by

$$A^T P + PA - \lambda_{\min}(H_{\min}) 2PBB^T P + k I_m = 0_{m \times m}. \tag{14}$$

Note that $\lambda_{\min}(H_{\min}) \triangleq \min\{\lambda_{\min}(H_{\text{sym}}(t))\} \in \mathbb{R}_{>0}$, such that $H_{\text{sym}}(t) \triangleq \frac{1}{2}(H(t) + H(t)^T) \in \mathbb{R}^{N \times N}$ and $k \geq k_1 + \frac{\rho^2}{\delta}$, where $\rho > 2\sqrt{N} M_0 S_{\max}(PB) \in \mathbb{R}_{>0}$, $k_1 \triangleq k_2 + k_3$, and $k_2, k_3, \delta \in \mathbb{R}_{>0}$ are user-defined parameters. Rather than use a traditional sample-and-hold event-triggered consensus control law such as in [20], the combined use of (10)–(13) enable each follower i to continuously compute a control input that evolves according to the leader's drift dynamics [44].

By using (1)–(3), (12), and (13), the time-derivative of (2) can be expressed as

$$\begin{aligned}\dot{e}_{1,i}(t) &= A e_{1,i}(t) - BK d_i(t) e_{1,i}(t) - BK d_i(t) e_{2,i}(t) \\ &\quad + BK \sum_{j \in \mathcal{N}_i(t)} a_{ij}(t) \left(e_{1,j}(t) - e_{1,i}(t)\right) \\ &\quad + BK \sum_{j \in \mathcal{N}_i(t)} a_{ij}(t) \left(e_{2,j}(t) - e_{2,i}(t)\right) \\ &\quad + BK e_{2,i}(t) - B u_0(t).\end{aligned} \tag{15}$$

Similarly, using (1)–(3), (10), (12), and (13), the weak time-derivative[6] of (3) can be expressed as

$$\begin{aligned}\dot{e}_{2,i}(t) &= A e_{2,i}(t) + BK d_i(t) e_{2,i}(t) + BK d_i(t) e_{1,i}(t) \\ &\quad - BK \sum_{j \in \mathcal{N}_i(t)} a_{ij}(t) \left(e_{2,j}(t) - e_{2,i}(t)\right) \\ &\quad - BK \sum_{j \in \mathcal{N}_i(t)} a_{ij}(t) \left(e_{1,j}(t) - e_{1,i}(t)\right) \\ &\quad - BK e_{2,i}(t).\end{aligned} \tag{16}$$

The stacked forms of (2) and (3) are defined as

$$e_1(t) \triangleq \left[e_{1,1}^T(t), e_{1,2}^T(t), \ldots, e_{1,N}^T(t)\right]^T \in \mathbb{R}^{mN}, \tag{17}$$

$$e_2(t) \triangleq \left[e_{2,1}^T(t), e_{2,2}^T(t), \ldots, e_{2,N}^T(t)\right]^T \in \mathbb{R}^{mN}, \tag{18}$$

respectively. Substituting (15) and (16) into the time-derivative of (17) and (18), respectively, and compactly expressing the results with the Kronecker product yields

$$\begin{aligned}\dot{e}_1(t) &= (I_N \otimes A) e_1(t) + ((I_N - H(t)) \otimes BK) e_2(t) \\ &\quad - (H(t) \otimes BK) e_1(t) - (1_N \otimes B u_0(t)),\end{aligned} \tag{19}$$

$$\begin{aligned}\dot{e}_2(t) &= (I_N \otimes (A - BK)) e_2(t) + (H(t) \otimes BK) e_2(t) \\ &\quad + (H(t) \otimes BK) e_1(t),\end{aligned} \tag{20}$$

respectively. The stacked form of (13) is defined by $z(t) \triangleq [z_1^T(t), z_2^T(t), \ldots, z_N^T(t)]^T \in \mathbb{R}^{mN}$. Substituting $\hat{x}(t) \triangleq [\hat{x}_1^T(t), \hat{x}_2^T(t), \ldots, \hat{x}_N^T(t)]^T \in \mathbb{R}^{mN}$ and (13) for all $i \in \mathcal{V}$ into $z(t)$ yields

$$z(t) = -(H(t) \otimes I_m) \hat{x}(t) + (D(t) \otimes I_m)(1_N \otimes x_0(t)). \tag{21}$$

Moreover, substituting (2), (3), and (13) for all $i \in \mathcal{V}$ into $z(t)$ yields

$$z(t) = -(H(t) \otimes I_m) e_2(t) - (H(t) \otimes I_m) e_1(t). \tag{22}$$

Since the objective is achieved when $e_{1,i}(t)$ is UUB for all cooperative followers $i \in \mathcal{V}$, it is sufficient to show that $e_1(t)$ is UUB. However, since $e_1(t)$ may contain error signals belonging to Byzantine followers, where the behavior of Byzantine followers cannot be controlled, the objective can only be guaranteed for the cooperative followers. Hence, if follower j is categorized as a Byzantine agent at t_k^j for some $k \in \mathbb{Z}_{\geq 0}$, then $e_{1,j}(t) \triangleq 0_m$ and $e_{2,j}(t) \triangleq 0_m$ for all $t \geq t_k^j$.

B. Stability Analysis

To facilitate the subsequent stability analysis, let

$$\gamma \triangleq \max\left\{\left\|(I_N - H(t)) \otimes 2PBB^T P\right\|\right\} \in \mathbb{R}_{>0},$$

$$\phi_1 \triangleq k_2 - \frac{\kappa(2k_3 + \gamma)}{2} \in \mathbb{R}_{>0},$$

$$\phi_2 \triangleq k_3 + \frac{2k_3 + \gamma}{2\kappa} \in \mathbb{R}_{>0},$$

$$\phi_3 \triangleq \frac{k_3}{\max\left\{\|H(t) \otimes I_m\|^2\right\}} \in \mathbb{R}_{>0},$$

[6]Weak time-derivative refers to the existence of the time-derivative for almost all time.

where $\kappa \in \mathbb{R}_{>0}$ is a user-defined parameter used in Young's inequality. Moreover, let $\bar{\delta} \triangleq \delta + \theta \in \mathbb{R}_{>0}$, where $\delta \in \mathbb{R}_{>0}$ is a user-defined parameter used to compensate for the effect of the leader's control input, and $\theta \in \mathbb{R}_{>0}$ is a user-defined parameter used to exclude Zeno behavior. Based on the definition of $\bar{\delta}$, we define additional constants, to facilitate the analysis, as

$$\beta_1 \triangleq \sqrt{\frac{\lambda_{\max}\left(I_N \otimes P\right)\bar{\delta}}{\lambda_{\min}\left(I_N \otimes P\right)\phi_1}} \in \mathbb{R}_{>0},$$

$$\beta_2 \triangleq \sqrt{\frac{V_1\left(e_1(0)\right)}{\lambda_{\min}\left(I_N \otimes P\right)}} \in \mathbb{R}_{\geq 0},$$

$$\beta_3 \triangleq \frac{\phi_1}{2\lambda_{\max}\left(I_N \otimes P\right)} \in \mathbb{R}_{>0}.$$

Given Assumption 2, the ARE in (14) has a positive definite solution P provided $\lambda_{\min}(H_{\min}) > 0$ [12], [44]. The following lemma shows $\lambda_{\min}(H_{\min}) > 0$.

Lemma 1: Suppose Assumptions 4–6 are satisfied. If all cooperative followers detect their Byzantine neighbors and employ (9), then $\lambda_{\min}(H_{\min}) > 0$.

Proof: See Appendix A. □

Theorem 1: The edge weight policy in (9), state observer in (10) and (11), and controller in (12) and (13) ensure the leader-follower error $e_1(t)$ is globally UBB as

$$\left\|e_1(t)\right\| \leq \beta_1 + \beta_2 e^{-\beta_3 t} \tag{23}$$

provided state feedback is available as dictated by the event-trigger in

$$t_{k+1}^i \triangleq \inf\left\{t > t_k^i : \phi_2\left\|e_{2,i}(t)\right\|^2 \geq \phi_3\left\|z_i(t)\right\|^2 + \frac{\theta}{N}\right\} \tag{24}$$

for all $i \in \mathcal{V}$, Assumptions 1–7 are satisfied, and the following sufficient user-defined parameter conditions are selected as follows: Use Algorithm 1 to determine P, and select $\kappa > 0$, $\delta > 0$, $\theta > 0$, $\rho > 2\sqrt{N}M_0 S_{\max}(PB)$, $k_3 > 0$, $k_2 > \frac{\kappa(2k_3+\gamma)}{2}$, and $k \geq k_1 + \frac{\rho^2}{\delta}$.

Proof: Consider the following candidate Lyapunov function $V_1 : \mathbb{R}^{mN} \to \mathbb{R}_{\geq 0}$ defined as:

$$V_1\left(e_1(t)\right) \triangleq e_1^T(t)\left(I_N \otimes P\right)e_1(t). \tag{25}$$

By the Rayleigh quotient,

$$\lambda_{\min}\left(I_N \otimes P\right)\left\|e_1(t)\right\|^2 \leq V_1\left(e_1(t)\right) \leq \lambda_{\max}\left(I_N \otimes P\right)\left\|e_1(t)\right\|^2. \tag{26}$$

Suppose $g : [0,\infty) \to \mathbb{R}^{mN}$ is a Filippov solution to the differential inclusion $\dot{g}(t) \in \overline{K}[h](g(t))$, where $g(t) = e_1(t)$, $\overline{K}[\cdot]$ is defined as in [45], and $h : \mathbb{R}^{mN} \to \mathbb{R}^{mN}$ is defined as $h(g(t)) = \dot{e}_1(t)$. The time-derivative of V_1 exists almost everywhere (a.e.), i.e., for almost all $t \in [0,\infty)$, and

$$\dot{V}_1\left(g(t)\right) \overset{a.e.}{\in} \dot{\tilde{V}}_1\left(g(t)\right), \tag{27}$$

where $\dot{\tilde{V}}_1(g(t))$ is the generalized time-derivative of V_1 along the Filippov trajectories of $\dot{g}(t) = h(g(t))$. By [46, eq. 13], $\dot{\tilde{V}}_1(g(t)) \triangleq \bigcap_{\xi\in\partial V_1(g(t))} \xi^T[\overline{K}[h]^T(g(t)), 1]^T$, where $\partial V_1(g(t))$ denotes the Clarke generalized gradient of $V_1(g(t))$. Since $V_1(g(t))$ is continuously differentiable in $g(t)$, $\partial V_1(g(t)) = \{\nabla V_1(g(t))\}$, where ∇ denotes the gradient operator. The generalized time-derivative of (25) is

$$\dot{\tilde{V}}_1\left(g(t)\right) \subseteq 2e_1^T(t)\left(I_N \otimes P\right)\overline{K}[h]\left(g(t)\right). \tag{28}$$

Using the calculus of $\overline{K}[\cdot]$ from [45] along with (28) and simplifying the substitution of (19) and $K = B^T P$ into the generalized time-derivative of (25) yields

$$\begin{aligned}\dot{\tilde{V}}_1\left(g(t)\right) \subseteq\ & \left\{e_1^T(t)\left(I_N \otimes \left(A^T P + PA\right)\right)e_1(t)\right\} \\ & - e_1^T(t)\overline{K}\left[H(t) \otimes 2PBB^T P\right]e_1(t) \\ & + e_1^T(t)\overline{K}\left[\left(\left(I_N - H(t)\right) \otimes 2PBB^T P\right)e_2(t)\right] \\ & - \left\{e_1^T(t)\left(1_N \otimes 2PBu_0(t)\right)\right\}.\end{aligned} \tag{29}$$

Let $M \triangleq H(t) \otimes 2PBB^T P \in \mathbb{R}^{mN\times mN}$, $M_{\text{sym}} \triangleq \frac{1}{2}(M + M^T) \in \mathbb{R}^{mN\times mN}$, and $M_{\text{skew}} \triangleq \frac{1}{2}(M - M^T) \in \mathbb{R}^{mN\times mN}$, where $M = M_{\text{sym}} + M_{\text{skew}}$. Since M_{skew} is a skew symmetric matrix, we see that $e_1^T(t)(H(t) \otimes 2PBB^T P)e_1(t) = e_1^T(t)M_{\text{sym}}e_1(t)$. It follows from the definition of M_{sym} that $e_1^T(t)M_{\text{sym}}e_1(t) = e_1^T(t)(H_{\text{sym}}(t) \otimes 2PBB^T P)e_1(t)$. Hence, $e_1^T(t)(H(t) \otimes 2PBB^T P)e_1(t) = e_1^T(t)(H_{\text{sym}}(t) \otimes 2PBB^T P)e_1(t)$. Since $H_{\text{sym}}(t)$ is a real, symmetric matrix, we then see that $H_{\text{sym}}(t)$ is diagonalizable, where there exists an orthogonal eigenvector matrix $T(t) \in \mathbb{R}^{N\times N}$ and eigenvalue matrix $\Lambda(t) \in \mathbb{R}^{N\times N}$, such that $H_{\text{sym}}(t) = T(t)\Lambda(t)T^T(t) \in \mathbb{R}^{N\times N}$. Hence, the eigendecomposition of $H_{\text{sym}}(t)$, the ARE, and (27) enable (29) to yield

$$\begin{aligned}\dot{V}_1\left(e_1(t)\right) \overset{a.e.}{\leq}\ & -ke_1^T(t)e_1(t) - e_1^T(t)\left(1_N \otimes 2PBu_0(t)\right) \\ & + e_1^T(t)\left(\left(I_N - H(t)\right) \otimes 2PBB^T P\right)e_2(t).\end{aligned} \tag{30}$$

Using Assumption 3 and selecting $k \geq k_1 + \frac{\rho^2}{\delta}$, equation (30) can be upper bounded by

$$\dot{V}_1\left(e_1(t)\right) \overset{a.e.}{\leq} -k_1\left\|e_1(t)\right\|^2 + \delta + \gamma\left\|e_2(t)\right\|\left\|e_1(t)\right\|. \tag{31}$$

Using (22), equation (31) can be further upper bounded by

$$\begin{aligned}\dot{V}_1\left(e_1(t)\right) \overset{a.e.}{\leq}\ & -\phi_1\left\|e_1(t)\right\|^2 + \bar{\delta} + \sum_{i\in\mathcal{V}}\Bigg[\phi_2\left\|e_{2,i}(t)\right\|^2 \\ & - \phi_3\left\|z_i(t)\right\|^2 - \frac{\theta}{N}\Bigg].\end{aligned} \tag{32}$$

By selecting $k_3 > 0$ and $k_2 > \frac{\kappa(2k_3+\gamma)}{2}$, $\phi_1 > 0$, $\phi_2 > 0$, and $\phi_3 > 0$. Based on (32), the event-trigger for each follower $i \in \mathcal{V}$ is given by (24). Hence, provided state feedback is available according to (24), it follows that:

$$\dot{V}_1\left(e_1(t)\right) \overset{a.e.}{\leq} -\phi_1\left\|e_1(t)\right\|^2 + \bar{\delta} \tag{33}$$

for all $t \geq 0$. Substituting (26) into (33) yields

$$\dot{V}_1\left(e_1(t)\right) \overset{a.e.}{\leq} -\frac{\phi_1}{\lambda_{\max}\left(I_N \otimes P\right)}V_1\left(e_1(t)\right) + \bar{\delta}. \tag{34}$$

Since the set of discontinuities as given by $\bigcup_{k\in\mathbb{Z}_{\geq 0}}\bigcup_{i\in\mathcal{V}}\{t_k^i\}$ is countable, $\dot{V}_1(e_1(t))$ and $V_1(e_1(t))$ are Lebesgue integrable over $\mathbb{R}_{\geq 0}$. The result in (23) then follows from (34) [47, Th. 2.5.1. Part V]. Observe that the constant β_1 can be made small, resulting in a small steady-state error for $e_1(t)$. Since $e_1(t) \in \mathcal{L}_\infty$ by (23), $e_{1,i}(t) \in \mathcal{L}_\infty$ for all $i \in \mathcal{C}(t)$. From Assumption 3, $x_0(t) \in \mathcal{L}_\infty$. By (2) and $x_0(t) \in \mathcal{L}_\infty$, $x_i(t) \in \mathcal{L}_\infty$ for each $i \in \mathcal{C}(t)$. Given (10) and (11), we see that $\hat{x}_i(t) = e^{A(t-t_k^i)}\hat{x}_i(t_k^i)$ over $t \in [t_k^i, t_{k+1}^i)$, where $\hat{x}_i(t_k^i) = x_i(t_k^i)$ for all $k \in \mathbb{Z}_{\geq 0}$. Therefore, $\hat{x}_i(t) \in \mathcal{L}_\infty$ for each $i \in \mathcal{C}(t)$, which then implies $e_{2,i}(t) \in \mathcal{L}_\infty$ by (3) for each $i \in \mathcal{C}(t)$. Hence, $u_i(t) \in \mathcal{L}_\infty$ for each $i \in \mathcal{C}(t)$. ■

Remark 3: There are two reasons why UUB stability is obtained rather than asymptotic stability. In (30), since

$$\begin{aligned} &-e_1^T(t)\left(1_N \otimes 2PBu_0(t)\right) \\ &\leq \|e_1(t)\| \, \|1_N \otimes 2PBu_0(t)\|, \end{aligned}$$

where $\|1_N \otimes 2PBu_0(t)\| \leq c$ for some $c \in \mathbb{R}_{>0}$ by Assumption 3, $-\left(1_N \otimes 2PBu_0(t)\right) e_1(t) \leq c\,\|e_1(t)\|$. Since the controller in (12)–(13) does not employ a sliding mode term or one of its variants, $c\|e_1(t)\|$ can only be compensated with high gain, which results in a residual $\delta > 0$. Note that it is not clear how to incorporate a sliding mode term into the controller in (12)–(13) since doing so would require $\text{sgn}(e_{1,i}(t))$ and $e_{1,i}(t)$ is not measurable by all followers. Next, the event-triggered strategy requires exclusion from Zeno behavior, which is accomplished by injecting $\theta > 0$ into (32), as shown in the proof of Theorem 2. Hence, the $\theta > 0$ term is combined with the residual $\delta > 0$ resulting in $\bar{\delta} = \delta + \theta$, and hence, UUB stability.

C. Exclusion of Zeno Behavior

Theorem 2: For each follower $i \in \mathcal{V}$, the difference between consecutive broadcast times generated by the event-trigger of follower i in (24) is uniformly lower bounded by

$$t_{k+1}^i - t_k^i \geq \frac{1}{\|A - BK\|} \ln\left(\frac{\|A - BK\|}{\|BK\|\,\bar{z}_i}\sqrt{\frac{\theta}{N\phi_2}} + 1\right) \tag{35}$$

for all $k \in \mathbb{Z}_{\geq 0}$.

Proof: Let $t \in [t_k^i, \infty)$. Substituting (1), (10), and (12) into the time-derivative of (3) yields $\dot{e}_{2,i}(t) = (A - BK)e_{2,i}(t) - BKz_i(t)$. Since $\|x_0(t)\| \leq \overline{M}_0$ by Assumption 3 and $\hat{x} \in \mathcal{L}_\infty$ by the proof of Theorem 1, equation (21) implies the existence of $\bar{z}_i \in \mathbb{R}_{>0}$, such that $\|z_i(t)\| \leq \bar{z}_i$ for all $t \in \mathbb{R}_{\geq 0}$. It then follows that:

$$\|\dot{e}_{2,i}(t)\| \leq \|A - BK\|\,\|e_{2,i}(t)\| + \|BK\|\,\bar{z}_i. \tag{36}$$

Let $\upsilon_i : [t_k^i, \infty) \to \mathbb{R}_{\geq 0}$ satisfy $\dot{\upsilon}_i(t) = \|A - BK\|\upsilon_i(t) + \|BK\|\bar{z}_i$ with initial condition $\upsilon_i(t_k^i) = \|e_{2,i}(t_k^i)\|$. Then, $\upsilon_i(t_k^i) = 0$ and

$$\upsilon_i(t) = \frac{\|BK\|\,\bar{z}_i}{\|A - BK\|}\left(e^{\|A-BK\|\left(t-t_k^i\right)} - 1\right). \tag{37}$$

Since $\frac{d}{dt}\|e_{2,i}(t)\| \overset{a.e.}{\leq} \|\dot{e}_{2,i}(t)\|$, equation (36) implies $\frac{d}{dt}\|e_{2,i}(t)\| \overset{a.e.}{\leq} \|A - BK\|\|e_{2,i}(t)\| + \|BK\|\bar{z}_i$, where $\|e_{2,i}(t)\| \leq \upsilon_i(t)$ for all $t \in [t_k^i, \infty)$. Since $\|e_{2,i}(t)\| \leq \upsilon_i(t)$ and $\|z_i(t)\| \geq 0$, equation (24) implies (35), where $\frac{1}{\|A-BK\|}\ln(\frac{\|A-BK\|}{\|BK\|\bar{z}_i}\sqrt{\frac{\theta}{N\phi_2}} + 1) > 0$ since $\frac{\|A-BK\|}{\|BK\|\bar{z}_i}\sqrt{\frac{\theta}{N\phi_2}} > 0$. ■

Remark 4: Since the event-trigger in (24) is free from Zeno behavior by the proof of Theorem 2, no follower continuously broadcasts state information about itself to its neighbors. Moreover, the difference between consecutive event-times can be made arbitrarily large by selecting a large θ. Since $\beta_1 = \sqrt{\frac{\lambda_{\max}(I_N \otimes P)\bar{\delta}}{\lambda_{\min}(I_N \otimes P)\phi_1}}$, where $\bar{\delta} = \delta + \theta$, selecting a large θ forces β_1 to be large as well. Hence, there is a tradeoff between the size of the neighborhood containing the cooperative followers and leader once approximate consensus is achieved and the amount of communication.

Remark 5: Define (37) over $[t_{k-1}^i, t_k^i)$, and observe that since $\|e_{2,i}(t)\| \leq \upsilon_i(t)$ over $[t_{k-1}^i, t_k^i)$, $\|e_{2,i}(t_k^i)\| = 0$, and $\upsilon_i(t)$ in (37) is strictly increasing, it follows that $\|e_{2,i}^-(t)\|$ defined in (5) satisfies the inequality $\|e_{2,i}^-(t)\| \leq \upsilon_i(t_k^i)$. Therefore, $\upsilon_i(t_k^i)$ is a candidate for $\Psi_{i,k}$.

Remark 6: If the event-trigger condition in (24) is satisfied for all $t \geq 0$, then

$$\phi_2\,\|e_{2,i}(t)\|^2 \leq \phi_3\,\|z_i(t)\|^2 + \frac{\theta}{N}.$$

Since $\|z_i(t)\| \leq \bar{z}_i$ for all $t \in \mathbb{R}_{\geq 0}$, substituting $\|z_i(t)\| \leq \bar{z}_i$ into $\phi_2\|e_{2,i}(t)\|^2 \leq \phi_3\|z_i(t)\|^2 + \frac{\theta}{N}$ yields

$$\|e_{2,i}(t)\| \leq \sqrt{\frac{\phi_3\bar{z}_i^2}{\phi_2} + \frac{\theta}{N\phi_2}} \in \mathbb{R}_{>0}.$$

Since $\|e_{2,i}(t)\| \leq \upsilon_i(t)$ for all $t \in [t_{k-1}^i, t_k^i)$, $\upsilon_i(t_k^i) > 0$, and $\|e_{2,i}(t_k^i)\| = 0$, $\|e_{2,i}(t)\| \leq \upsilon_i(t)$ for all $t \in [t_{k-1}^i, t_k^i]$. Since $\upsilon_i(t)$ will reach $\sqrt{\frac{\phi_3\bar{z}_i^2}{\phi_2} + \frac{\theta}{N\phi_2}}$ before or at the same time as $\|e_{2,i}(t)\|$, we then see that $\frac{\|BK\|\bar{z}_i}{\|A-BK\|}(e^{\|A-BK\|(t_k^i - t_{k-1}^i)} - 1) \leq \sqrt{\frac{\phi_3\bar{z}_i^2}{\phi_2} + \frac{\theta}{N\phi_2}}$ implies $t_k^i \leq t_{k-1}^i + \Delta_{i,\min}$, where

$$\Delta_{i,\min} \triangleq \frac{1}{\|A - BK\|}\ln\left(\frac{\|A - BK\|}{\|BK\|\,\bar{z}_i}\sqrt{\frac{\phi_3\bar{z}_i^2}{\phi_2} + \frac{\theta}{N\phi_2}} + 1\right) \tag{38}$$

and $\Delta_{i,\min} \in \mathbb{R}_{>0}$. Hence, $\|e_{2,i}(t)\| \leq \sqrt{\frac{\phi_3\bar{z}_i^2}{\phi_2} + \frac{\theta}{N\phi_2}}$ for all $t \geq 0$ provided $t_k^i \leq t_{k-1}^i + \Delta_i$ for each $k \in \mathbb{Z}_{>0}$, where Δ_i is a user-defined parameter to be selected, such that $\Delta_i \geq \Delta_{i,\min}$. Note that an analytical upper bound for Δ_i requires the derivation of a nonzero lower bound for $\|e_{2,i}(t)\|$, which is not obvious.

Algorithm 1 presents a method for parameter selection.

VII. Self-Triggered Control

When the trigger condition in (24) is true, follower i will broadcast its state to each follower $j \in \mathcal{N}_i(t)$ to reset (3) and ensure (33). Such an ETC strategy requires follower i to continuously monitor (24) and for each follower $j \in \mathcal{N}_i(t)$ to continuously sense for follower i's broadcast. An STC strategy is developed in this section, where follower i determines and reports to its neighbors the future time when its own trigger condition will become true, eliminating the need for followers to continuously monitor for a neighbor's broadcast.

Based on (32), stability is preserved when $\phi_2\|e_{2,i}(t)\|^2 - \phi_3\|z_i(t)\|^2 - \frac{\theta}{N} \leq 0$ for each $i \in \mathcal{V}$. Since $\phi_3 > 0$ and

Algorithm 1: Parameter Selection Protocol.

Select $\delta, \kappa, \theta, k, k_3 \in \mathbb{R}_{>0}$.
Compute $\bar{\delta} = \delta + \theta$.
Compute $\lambda_{\min}(H_{\min}) = \min\{\lambda_{\min}(H_{\text{sym}}(t))\}$.
while true **do**
  Compute P from (14).
  Select $\rho > 2\sqrt{N}M_0 S_{\max}(PB)$.
  Compute $\gamma = \max\{\|(I_N - H(t)) \otimes 2PBB^T P\|\}$.
  Select $k_2 > \frac{\kappa(2k_3+\gamma)}{2}$.
  Compute $k_1 = k_2 + k_3$.
  if $k_1 + \frac{\rho^2}{\delta} \leq k$ **then**
    break
  else
    $k = k_1 + \frac{\rho^2}{\delta}$.
  end if
end while
Compute $K = B^T P$.
Compute $\phi_1 = k_2 - \frac{\kappa(2k_3+\gamma)}{2}$.
Compute $\phi_2 = k_3 + \frac{2k_3+\gamma}{2\kappa}$.
Compute $\phi_3 = \frac{k_3}{\max\{\|H(t)\otimes I_m\|^2\}}$.

$\|z_i(t)\| \geq 0$, $\phi_3\|z_i(t)\|^2 \geq 0$, where stability is preserved provided $\phi_2\|e_{2,i}(t)\|^2 - \frac{\theta}{N} \leq 0$ for each $i \in \mathcal{V}$. While triggering based on $\phi_2\|e_{2,i}(t)\|^2 - \frac{\theta}{N} \geq 0$ results in more conservative event-times for follower i than when triggering based on $\phi_2\|e_{2,i}(t)\|^2 - \phi_3\|z_i(t)\|^2 - \frac{\theta}{N} \geq 0$, the former results in a simpler condition from which to develop a self-trigger. Let t_k^i mark the k^{th} instance when $\phi_2\|e_{2,i}(t)\|^2 - \frac{\theta}{N} \geq 0$. Hence, an event for follower i occurs at t_k^i provided $\phi_2\|e_{2,i}(t_k^i)\|^2 - \frac{\theta}{N} \geq 0$. Note that for $t \in [t_k^i, t_{k+1}^i)$, $\phi_2\|e_{2,i}(t)\|^2 - \frac{\theta}{N} \leq 0$ since $\|e_{2,i}(t_k^i)\| = 0$ and $\|e_{2,i}(t)\|$ may increase otherwise.

Substituting (1) and (10) into the time-derivative of (3) yields

$$\dot{e}_{2,i}(t) = Ae_{2,i}(t) - Bu_i(t). \tag{39}$$

The evolution of (3) is governed by (39), where the solution to (39) is not available since $u_i(t)$ is unknown *a priori*. Therefore, follower i cannot determine its own event-times. Let $\breve{e}_{2,i} : [0,\infty) \to \mathbb{R}_{\geq 0}$ denote an estimate of $\|e_{2,i}(t)\|$, and let $\{\hat{t}_k^i\}_{k=1}^{\infty} \subset \mathbb{R}_{\geq 0}$ be an increasing sequence of estimated event-times determined by a subsequently developed self-trigger for follower i. The estimate $\breve{e}_{2,i}(t)$ is designed, such that

$$\phi_2\|e_{2,i}(t)\|^2 - \frac{\theta}{N} \leq \phi_2 \breve{e}_{2,i}^2(t) - \frac{\theta}{N} \tag{40}$$

holds for all $t \in [t_k^i, t_{k+1}^i)$. Hence, executing the consensus protocol based on the estimated event-times originating from a self-trigger using $\breve{e}_{2,i}(t)$ for all $i \in \mathcal{V}$ ensures the stability of the MAS. Based on the subsequent stability analysis, for each $[t_k^i, t_{k+1}^i)$, the estimate $\breve{e}_{2,i}(t)$ is designed as

$$\breve{e}_{2,i}(t) \triangleq \xi_i\left(e^{S_{\max}(A)\left(t-t_k^i\right)} - 1\right), \tag{41}$$

$$\xi_i \triangleq \frac{S_{\max}(B)M_i}{S_{\max}(A)} \in \mathbb{R}_{>0}. \tag{42}$$

In (42), $M_i \in \mathbb{R}_{>0}$ is a known upper bound for $\|u_i(t)\|$, which exists given the proof of Theorem 1. Furthermore, Lemma 2 provides an upper bound for $\|u_i(t)\|$.

Lemma 2: If the conditions in Theorem 1 are satisfied, then for each $i \in \mathcal{C}(t)$ and all $t \geq 0$

$$\begin{aligned}\|u_i(t)\| \leq{}& S_{\max}\left(B^T P\right)\max\{\|H(t)\otimes I_m\|\}\sqrt{\frac{\theta}{\phi_2}}\\ &+ S_{\max}\left(B^T P\right)\max\{\|H(t)\otimes I_m\|\}(\beta_1+\beta_2)\\ &+ S_{\max}\left(B^T P\right)\sqrt{\frac{\theta}{N\phi_2}}.\end{aligned} \tag{43}$$

Proof: See Appendix B.

Theorem 3: The estimate given by (41) and (42) satisfies (40) for all $t \in [t_k^i, t_{k+1}^i)$, where $\hat{t}_{k+1}^i \leq t_{k+1}^i$, such that $\hat{t}_{k+1}^i$ originates from the self-trigger given by

$$\hat{t}_{k+1}^i \triangleq \inf\left\{t > \hat{t}_k^i : \phi_2 \breve{e}_{2,i}(t)^2 \geq \frac{\theta}{N}\right\}. \tag{44}$$

Proof: To satisfy (40), it is equivalent to show that $\breve{e}_{2,i}(t) \geq \|e_{2,i}(t)\|$ for all $t \in [t_k^i, t_{k+1}^i)$. Let $t \in [t_k^i, t_{k+1}^i)$. A Lyapunov-like function $V_{2,i} : \mathbb{R}^m \to \mathbb{R}_{\geq 0}$ is defined as

$$V_{2,i}\left(e_{2,i}(t)\right) \triangleq \frac{1}{2}e_{2,i}^T(t)e_{2,i}(t), \tag{45}$$

which is continuously differentiable over $t \in [t_k^i, t_{k+1}^i)$. Substituting (39) into the time-derivative of (45) results in

$$\begin{aligned}\dot{V}_{2,i}\left(e_{2,i}(t)\right) \leq{}& S_{\max}(A)\left\|e_{2,i}(t)\right\|^2\\ &+ S_{\max}(B)\left\|e_{2,i}(t)\right\|\left\|u_i(t)\right\|.\end{aligned} \tag{46}$$

Based on the proof of Theorem 1, $u_i(t) \in \mathcal{L}_\infty$, where $\|u_i(t)\| \leq M_i$, such that M_i is a known bounding constant. Hence, equation (46) can be upper bounded by

$$\begin{aligned}\dot{V}_{2,i}\left(e_{2,i}(t)\right) \leq{}& 2S_{\max}(A)V_{2,i}\left(e_{2,i}(t)\right)\\ &+ S_{\max}(B)M_i\sqrt{2V_{2,i}\left(e_{2,i}(t)\right)}.\end{aligned} \tag{47}$$

Since follower i broadcasts its state at t_k^i, $V_{2,i}(e_{2,i}(t_k^i)) = 0$. Invoking the Comparison lemma in [48, Lemma 3.4] on (47) yields

$$V_{2,i}\left(e_{2,i}(t)\right) \leq \left(\frac{\sqrt{2}\xi_i\left(e^{S_{\max}(A)\left(t-t_k^i\right)} - 1\right)}{2}\right)^2. \tag{48}$$

Substituting (45) into (48) yields $\|e_{2,i}(t)\| \leq \xi_i(e^{S_{\max}(A)(t-t_k^i)} - 1) = \breve{e}_{2,i}(t)$. Hence, equation (40) holds for all $t \in [t_k^i, t_{k+1}^i)$, where the conditions in (24) and (44) imply $\hat{t}_{k+1}^i \leq t_{k+1}^i$.[7] ■

Remark 7: The self-trigger condition in (44) is free from Zeno behavior by a similar argument provided in the proof of Theorem 2.

Remark 8: Define (41) over $[t_{k-1}^i, t_k^i)$, and observe that since $\|e_{2,i}(t)\| \leq \breve{e}_{2,i}(t)$ over $[t_{k-1}^i, t_k^i)$, $\|e_{2,i}(t_k^i)\| = 0$, and $\breve{e}_{2,i}(t)$ in (41) is strictly increasing, it follows that $\|e_{2,i}^-(t)\|$ defined in (5) satisfies the inequality $\|e_{2,i}^-(t)\| \leq \breve{e}_{2,i}(t_k^i)$. Therefore, $\breve{e}_{2,i}(t_k^i)$ is a candidate for $\Psi_{i,k}$.

[7]While (41) is initialized at t_k^i in the development, implementation of the STC strategy requires communication at $\hat{t}_k^i$.

VIII. Simulation Study

A simulation study is included to demonstrate and compare the performances of the developed approaches. The simulated MAS consists of five follower agents and a single leader agent. The initial positions of each agent, which are equivalent for all simulations, are $x_0(0) = [6, 2]^T$ m, $x_1(0) = [12, 2.5]^T$ m, $x_2(0) = [12, 2]^T$ m, $x_3(0) = [12, 1.5]^T$ m, $x_4(0) = [13, 2.25]^T$ m, and $x_5(0) = [13, 1.75]^T$ m. The known state and control effectiveness matrices used in all simulations are given by

$$A \triangleq \begin{bmatrix} 0.05 & 0 \\ 0 & 0 \end{bmatrix}, \; B \triangleq \begin{bmatrix} 0.3 & 0 \\ 0 & 0.3 \end{bmatrix}.$$

The known desired trajectory $x_d : [0, \infty) \to \mathbb{R}^2$ of the leader is

$$x_d(t) \triangleq [5\cos(0.2\pi t), 5\sin(0.4\pi t)]^T, \tag{49}$$

while the leader's trajectory tracking error $e_0 : [0, \infty) \to \mathbb{R}^2$ is

$$e_0(t) \triangleq x_d(t) - x_0(t). \tag{50}$$

The leader's tracking error in (50) can be globally exponentially regulated using the following controller:

$$u_0(t) \triangleq B^{-1}(\dot{x}_d(t) - Ax_0(t) + k_0 e_0(t)), \tag{51}$$

where $k_0 > 0$.

Lemma 3: The controller of the leader provided in (51) ensures (50) is globally exponentially regulated and $x_0, u_0 \in \mathcal{L}_\infty$ provided the desired trajectory satisfies $x_d, \dot{x}_d \in \mathcal{L}_\infty$, Assumption 1 is satisfied, the right pseudo inverse of the control effectiveness matrix, i.e., B, exists, and k_0 is selected, such that $k_0 > 0$.

Proof: See Appendix C.

All simulations are 12-s long and use an integration time-step of 1.00×10^{-5} s. Additionally, all ETC and STC simulations used the following parameters, which originate from Algorithm 1: $k_0 = 3\text{s}^{-1}, \delta = 3 \times 10^7, \kappa = 1.00 \times 10^{-2}, \rho = 4.87 \times 10^5, \gamma = 1.54 \times 10^5, k_1 = 2.78 \times 10^3, k_2 = 1.78 \times 10^3, k_3 = 1.00 \times 10^3, \; k = 1.07 \times 10^4, \; \theta = 1.00 \times 10^3 \text{ m}^2 \cdot s^{-1}, \; \phi_1 = 1.00 \times 10^3 \text{ s}^{-1}, \phi_2 = 7.80 \times 10^6 \text{ s}^{-1}, \phi_3 = 37.87 \text{ s}^{-1}, M_1 = 800$ m, $M_2 = 800$ m, $M_3 = 800$ m, $M_4 = 800$ m, and $M_5 = 800$ m.

A. Benchmark Simulation

As a benchmark, the MAS is first simulated by using an event-triggered approach, where all followers are designed as cooperative agents for the entire simulation. The network used in the benchmark simulation is depicted by the left topology in Fig. 1, and Figs. 2 and 3 display the results.

Fig. 2 displays a planar view of the MAS trajectories for the ETC method with cooperative agents. Fig. 3 presents the norm of the tracking errors of the followers and leader as quantified by (2) and (50), respectively. In Fig. 3, the followers connected to the leader experience smaller tracking errors than the followers that are not connected to the leader. The maximum steady-state tracking errors of Followers 1–5 are 0.41, 0.46, 0.68, 0.59, and 0.72 m, respectively. Moreover, the maximum steady-state velocities of Followers 1–5 are 7.38, 7.34, 7.27, 7.39, and 7.22 m/s, respectively. The time instances a follower sent information to a neighbor were measured throughout the simulation. The minimum time difference between consecutive communication

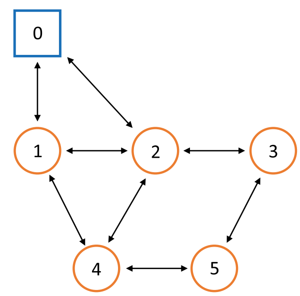

Fig. 1. Illustration of the network topologies used in simulations. The network on the left consists only of cooperative followers while the network on the right consists of both cooperative and Byzantine followers. The blue square denotes the leader agent, the orange circles denote the cooperative followers, and the red triangles denote the Byzantine followers.

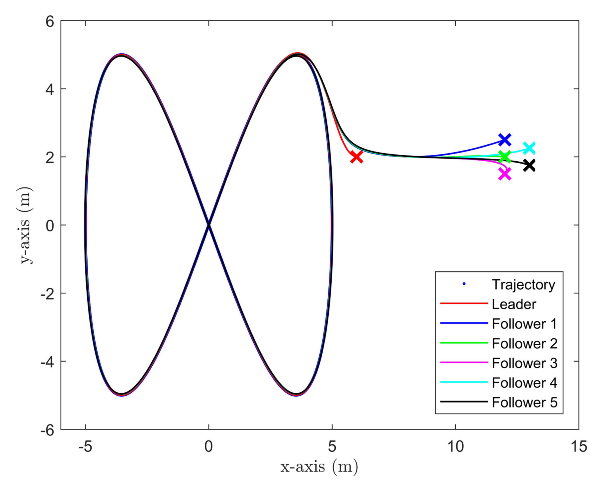

Fig. 2. Planar trajectories of the MAS using an event-triggered approach. The x's denote the starting position of each agent.

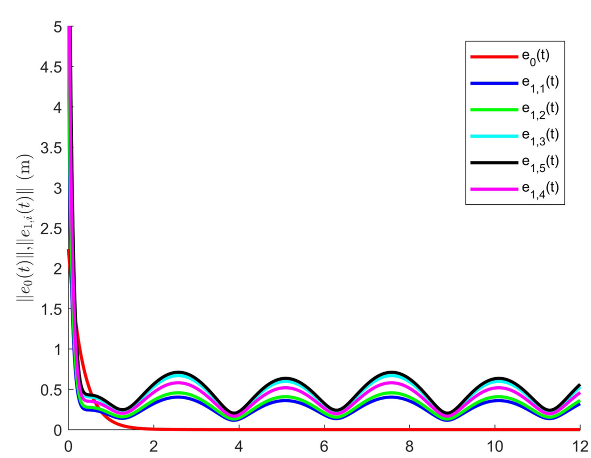

Fig. 3. Norm of tracking errors for the MAS using the ETC approach. All followers are cooperative agents.

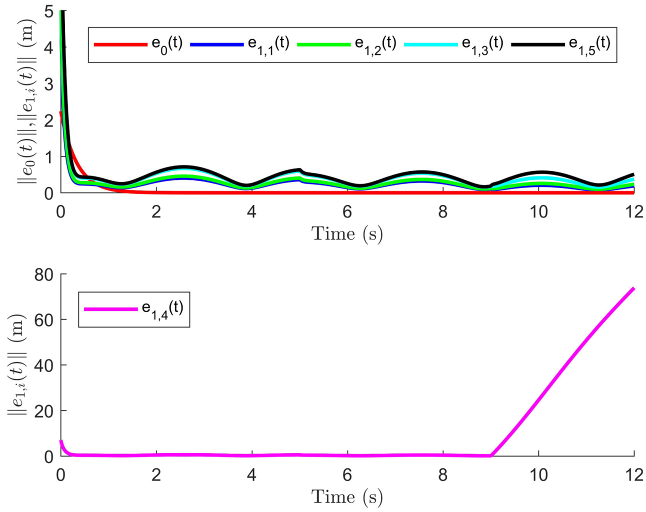

Fig. 4. Norm of tracking errors for the MAS using the ETC approach. Follower 4 is a Type II Byzantine agent, and Follower 5 is a Type I Byzantine agent.

instances for all followers was 6.00×10^{-5} s, which implies that all followers must be equipped with radios capable of broadcasting at approximately 16.67 kHz.

B. ETC Simulation With Byzantine Adversaries

The next simulation is similar to the benchmark, except two originally cooperative followers are converted into Byzantine agents. Specifically, Follower 4 is converted into a Type II Byzantine agent at time $t = 9$ s, and Follower 5 is converted into a Type I Byzantine agent at time $t = 5$ s. For $t \geq 9$ s, Follower 4 executes the controller $u_4(t) = [50, -50]^T$, and for $t \geq 5$ s, Follower 5 communicates state information about itself to its neighbors according to $x_{5,i}(t) = e^{100 I_2(t-5)} x_5(t)$, where $x_{5,i}(t)$ denotes the position of Follower 5 within the global coordinate frame at time $t \geq 5$ that is communicated to neighbor i. The objective of the remaining cooperative followers is to identify any potential Byzantine neighbors, remove the Byzantine agent's influence from their controllers, and synchronize their trajectories to the leader's trajectory. Successful execution of this protocol will transform the communication topology from the left network to the right network in Fig. 1.

Fig. 4 demonstrates that the cooperative followers satisfied the objective, where Followers 1 and 2 each detected the Type II Byzantine agent at $t = 9.04$ s and Follower 3 detected the Type I Byzantine agent at $t = 5.02$ s. As seen in Fig. 4, the followers connected to the leader experience smaller tracking errors than followers that are not connected to the leader. The maximum steady-state tracking errors of Followers 1–3 are 0.41, 0.46, and 0.68 m, respectively. Moreover, the maximum steady-state velocities of Followers 1–3 are 7.58, 7.75, 11.57 m/s, respectively. The minimum time difference between consecutive communication instances for all followers was 6.00×10^{-5} s. Followers 4 and 5 are Byzantine adversaries, where their behaviors cannot be guaranteed. Therefore, their steady-state tracking error and maximum steady-state velocity are not included. When compared to the benchmark simulation results, the cooperative followers in this simulation obtain the same steady-state tracking errors and similar maximum steady-state velocities. Therefore, the ETC method obtained similar performance to the benchmark result.

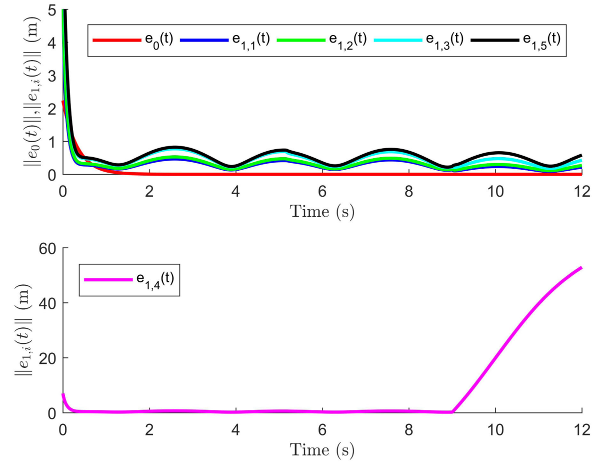

Fig. 5. Norm of tracking errors for the MAS using the STC approach. Follower 4 is a Type II Byzantine agent, and Follower 5 is a Type I Byzantine agent.

C. STC Simulation With Byzantine Adversaries

This simulation is identical to the one in Section VIII-B, except the STC method from Section VII is used instead. Fig. 5 demonstrates that the cooperative followers satisfied the objective, where Followers 1 and 2 detected the Type II Byzantine agent at $t = 9.001$ s and Follower 3 detected the Type I Byzantine agent at $t = 5.001$ s. As depicted in Fig. 5, the followers connected to the leader experience smaller tracking errors than followers that are not connected to the leader. The maximum steady-state tracking errors of Followers 1–3 are 0.40, 0.46, and 0.67 m, respectively. Moreover, the maximum steady-state velocities of Followers 1–3 are 7.25, 7.31, 7.70 m/s, respectively. The minimum time difference between consecutive communication instances for all followers was 2.00×10^{-5} s.

When compared to the ETC results with Byzantine agents, the cooperative followers in the STC simulation obtain similar steady-state tracking errors and maximum steady-state velocities. While the same θ parameter was used between simulations, further investigation of the effect θ has on communication is needed for the ETC and STC approaches. The results of such a study are provided in the following subsection.

D. Communication Frequency Versus Performance Study

In this section, six simulations are performed for the ETC and STC strategies under the same parameters as the previous simulations, except θ is varied to investigate the tradeoff between communication frequency and steady-state consensus errors. Furthermore, an additional reference simulation is performed to enable comparison between the ETC and STC results. The reference simulation is performed under the same parameters as

TABLE I
ETC COMMUNICATION-PERFORMANCE SUMMARY

Simulation	1	2	3	4	5	6
$\theta(\ m^2 \cdot s^{-1})$	1.00×10^3	1.00×10^4	1.00×10^5	1.00×10^6	1.00×10^7	1.00×10^8
$\beta_{1,m}\ \ (m)$	0.68	0.69	0.78	0.81	0.86	1.15
Min. Comm. Time (s)	6.00×10^{-5}	1.00×10^{-4}	2.60×10^{-4}	2.90×10^{-4}	8.30×10^{-4}	6.70×10^{-3}
Comm. Max. Energy (J)	1.45×10^3	467.04	148.96	54.17	53.63	28.89
Follower 1: Comm. Fraction	0.17	0.06	0.02	0.01	0.007	0.004
Follower 2: Comm. Fraction	0.27	0.09	0.03	0.01	0.009	0.003
Follower 3: Comm. Fraction	0.19	0.06	0.02	0.01	0.007	0.004
Follower 4: Comm. Fraction	0.25	0.08	0.03	0.01	0.009	0.005
Follower 5: Comm. Fraction	0.17	0.06	0.02	0.01	0.006	0.002*

TABLE II
STC COMMUNICATION-PERFORMANCE SUMMARY

Simulation	1	2	3	4	5	6
$\theta(\ m^2 \cdot s^{-1})$	1.00×10^3	1.00×10^4	1.00×10^5	1.00×10^6	1.00×10^7	1.00×10^8
$\beta_{1,m}\ \ (m)$	0.67	0.67	0.67	0.67	0.69	0.74
Min. Comm. Time (s)	2.00×10^{-5}	6.00×10^{-5}	2.10×10^{-4}	6.60×10^{-4}	2.10×10^{-3}	3.20×10^{-3}
Comm. Max. Energy (J)	7.49×10^4	2.37×10^4	7.50×10^3	2.37×10^3	749.90	237.22
Follower 1: Comm. Fraction	8.28	2.62	0.83	0.26	0.08	0.03
Follower 2: Comm. Fraction	13.02	4.12	1.30	0.41	0.13	0.04
Follower 3: Comm. Fraction	9.47	2.99	0.95	0.30	0.09	0.03
Follower 4: Comm. Fraction	11.83	3.74	1.18	0.37	0.12	0.04
Follower 5: Comm. Fraction	8.28	2.62	0.83	0.26	0.08	0.03

the previous simulations except all agents communicate at the same fixed rate of 10 kHz. A communication rate of 10 kHz for a 12-s simulation results in 1.20×10^5 reference event-times, i.e., reference communication instances. Tables I and II summarize the results of the ETC and STC simulations, respectively, where $\beta_{1,m}$ denotes the maximum steady-state tracking error between Followers 1–3, Min. Comm. Time denotes the minimum time difference between consecutive communication events over all followers, Comm. Fraction represents the amount of communication performed by an agent as determined by

$$\text{Comm. Fraction} \triangleq \frac{\text{Number of Event Times}}{\text{Number of Ref. Event Times}}, \tag{52}$$

and Comm. Max. Energy denotes the maximum amount of energy used by all followers to monitor and transmit data. According to [49], the energy $J_i : [0, \infty) \to \mathbb{R}_{\geq 0}$ consumed by follower i at time t to monitor and transmit data under an ETC approach is given by $J_i(t) \triangleq \sum_{k \in \Gamma_i(t)} (c_1 + p_2 c_2) + c_3 t$, where $\Gamma_i(t) \triangleq \{k : t_k^i \leq t\}$, c_1 describes the cost associated to the packet overhead transmission, c_2 describes the cost per transmitted scalar, c_3 describes the cost of continuous monitoring, and p_2 denotes the number of transmitted scalars. Since the STC method does not require continuous monitoring of the trigger condition, where monitoring is done at the same time as transmission, the monitoring cost is negligible when compared to the ETC approach. Therefore, the energy consumption function for follower i using STC is $J_i(t) \triangleq \sum_{k \in \Gamma_i(t)} (c_1 + p_2 c_2)$. The parameters c_1 through c_3 denote fixed energy costs consumed per update. Since each follower transmits its state at the current event-time under the ETC approach, $p_2 = 2$ given $x_i(t) \in \mathbb{R}^2$. For STC, each follower transmits its state and future event-time at the current event-time. Hence, $p_2 = 3$ since $x_i(t) \in \mathbb{R}^2$ and $t_k^i \in \mathbb{R}_{\geq 0}$. The parameters used in the energy consumption functions are $c_1 = 38.4$ mJ, $c_2 = 3.2$ mJ, and $c_3 = 60$ mW, which are approximations obtained from power consumption values for a MicaZ using a ZigBee for wireless communication [49].

The * next to the Comm. Fraction of Follower 5 in Table I indicates that Follower 5 was not able to detect Follower 4 as a Byzantine neighbor. As seen in Tables I and II, frequent communication results in high-energy costs. Moreover, frequent communication leads to better tracking performance, where the cooperative followers can track the leader more closely.

Tables I and II also indicate that the STC approach yields better performance than the ETC strategy relative to the same value of θ because of the more frequent communication by STC than ETC. However, ETC can yield comparable performance to STC while using less energy to communicate.

IX. Conclusion

In this work, the approximate leader-follower consensus problem in the presence of Byzantine adversaries for a homogeneous MAS is examined. Distributed event- and self-triggered controllers are developed along with a Lyapunov-based detection method that enables followers to discern between cooperative and Byzantine neighbors. The controllers can remove the influence from Byzantine agents by altering the interaction topology and enabling consensus for all cooperative followers. Moreover, a time-based estimate for each follower's trigger condition is developed, which allows each follower to estimate the future time when state information from its neighbors will be required. The STC approach alleviates the continuous monitoring requirement of ETC and enables intermittent communication and monitoring. Future efforts could focus on generalizing the result to more abstract network topologies, developing more capable and sensitive Byzantine detection and trigger condition estimation methods, and relaxing Assumption 5 by developing a controller capable of ensuring network connectivity maintenance in the presence of Byzantine adversaries. Moreover, uncertain agent dynamics can be considered, the impact of which leads to faster divergence rates between the estimated and true follower position, and more frequent triggering and communication. Simulation results demonstrate that both ETC and STC methods enable approximate leader-follower consensus while identifying and mitigating against Byzantine adversaries. Results also show that increased communication leads to better tracking of the leader for both ETC and STC. Moreover, both methods can provide identical tracking performance, but depending on the choice of parameters, one method can provide communication energy savings over the other.

Appendix

A. Proof of Lemma 1

Proof: Assume the hypothesis of Lemma 1, and fix $t_1 \geq 0$. By Assumptions 5 and 6, $H(t_1)$ is a diagonally dominant matrix, where each row of $H(t_1)$ is nonzero. By Assumptions 4 and 5, $H(t_1)$ contains a strictly diagonally dominant row, i.e., $|H_{ii}(t_1)| > \sum_{j\in\mathcal{V}, j\neq i} |H_{ij}(t_1)|$ for some $i \in \mathcal{V}$. Claim: If $H(t_1)$ is a diagonally dominant matrix with a strictly diagonally dominant row, then $H_{\text{sym}}(t_1)$ is a symmetric, diagonally dominant matrix with a strictly diagonally dominant row. Suppose the claim is true. Therefore, $H_{\text{sym}}(t_1)$ is a symmetric, diagonally dominant matrix with a strictly diagonally dominant row. Since $I_N + |H_{\text{sym}}(t_1)|$ is a symmetric, strictly diagonally dominant matrix, $I_N + |H_{\text{sym}}(t_1)|$ is positive definite by the Gershgorin disk theorem in [9, Th. 3.9.]. Let $\{\lambda_i\}_{i=1}^N \subset \mathbb{R}_{>0}$ denote the eigenvalues of $I_N + |H_{\text{sym}}(t_1)|$. Since $\lambda_i \in \mathbb{R}_{>0}$ for all $i \in \mathcal{V}$, and the eigenvalues of $(I_N + |H_{\text{sym}}(t_1)|)^{N-1}$ are $\{\lambda_i^{N-1}\}_{i=1}^N$, $\lambda_i^{N-1} \in \mathbb{R}_{>0}$ for each $i \in \mathcal{V}$. Since $(I_N + |H_{\text{sym}}(t_1)|)^{N-1}$ is a symmetric matrix with positive eigenvalues, $(I_N + |H_{\text{sym}}(t_1)|)^{N-1}$ is positive definite. Hence, $H_{\text{sym}}(t_1)$ is irreducible by [50, Theorem 6.2.24.]. Since $H_{\text{sym}}(t_1)$ is an irreducible, diagonally dominant matrix with a strictly diagonally dominant row, $H_{\text{sym}}(t_1)$ is irreducibly diagonally dominant by [50, Definition 6.2.25.]. Since $H_{\text{sym}}(t_1)$ is irreducibly diagonally dominant, $H_{\text{sym}}(t_1)$ is nonsingular [50, Corollary 6.2.27.], i.e., $\lambda_{\min}(H_{\text{sym}}(t_1)) > 0$. Since t_1 is arbitrary, $\lambda_{\min}(H_{\text{sym}}(t)) > 0$ for all $t \geq 0$. Since $\{\lambda_{\min}(H_{\text{sym}}(t)) : \forall t \geq 0\}$ is a finite set, $\lambda_{\min}(H_{\min}) \triangleq \min\{\lambda_{\min}(H_{\text{sym}}(t))\} \in \mathbb{R}_{>0}$ is well defined.

Proof of Claim: Let $H(t_1)$ be a diagonally dominant matrix, i.e., row diagonally dominant, where $|H_{ii}(t_1)| \geq \sum_{j\neq i} |H_{ij}(t_1)|$ for all $i \in \mathcal{V}$. Then, $H(t_1)^T$ is a column diagonally dominant matrix, where $|H_{ii}(t_1)| \geq \sum_{j\neq i} |H_{ji}(t_1)|$ for all $i \in \mathcal{V}$. Recall that $H_{\text{sym}}(t_1) = \frac{1}{2}(H(t_1) + H(t_1)^T)$. Then, for fixed $i \in \mathcal{V}$, it follows that:

$$\begin{aligned}\sum_{j\neq i} |H_{\text{sym},ij}| &= \sum_{j\neq i} \left|\frac{1}{2}\left(H_{ij}(t_1) + H_{ji}(t_1)\right)\right| \\ &= \frac{1}{2}\sum_{j\neq i} |H_{ij}(t_1) + H_{ji}(t_1)| \\ &\leq \frac{1}{2}\sum_{j\neq i} \left(|H_{ij}(t_1)| + |H_{ji}(t_1)|\right) \\ &\leq |H_{ii}(t_1)| \\ &= |H_{\text{sym},ii}(t)|.\end{aligned}$$

Since $\sum_{j\neq i} |H_{\text{sym},ij}| \leq |H_{\text{sym},ii}(t)|$ for each $i \in \mathcal{V}$, $H_{\text{sym}}(t_1)$ is diagonally dominant. The existence of a strictly diagonally dominant row/column follows by a similar argument. ■

B. Proof of Lemma 2

Proof: Let $t \geq 0$. Given (12) and $K = B^T P$, it follows that

$$\|u_i(t)\| \leq S_{\max}\left(B^T P\right)\|z_i(t)\| + S_{\max}\left(B^T P\right)\|e_{2,i}(t)\|. \tag{53}$$

Provided the self-trigger in (44) is satisfied for all $t \geq 0$, $\phi_2\|e_{2,i}(t)\|^2 - \frac{\theta}{N} \leq 0$ for all $t \geq 0$ by Theorem 3, where

$$\|e_{2,i}(t)\| \leq \sqrt{\frac{\theta}{N\phi_2}}. \tag{54}$$

By (22), it follows that:

$$\|z(t)\| \leq \max\left\{\|H(t) \otimes I_m\|\right\}\left(\|e_2(t)\| + \|e_1(t)\|\right). \tag{55}$$

Since $\|e_1(t)\| \leq \beta_1 + \beta_2 e^{-\beta_3 t}$ for all $t \geq 0$ by Theorem 1

$$\|e_1(t)\| \leq \beta_1 + \beta_2. \tag{56}$$

Substituting (54) into $\|e_2(t)\|^2 = \sum_{i\in\mathcal{V}} \|e_{2,i}(t)\|^2$ implies

$$\|e_2(t)\| \leq \sqrt{\frac{\theta}{\phi_2}}. \tag{57}$$

Since $\|z_i(t)\| \leq \|z(t)\|$, (55) implies

$$\|z_i(t)\| \leq \max\left\{\|H(t) \otimes I_m\|\right\}\left(\|e_2(t)\| + \|e_1(t)\|\right). \tag{58}$$

Substituting (54), (56), (57), and (58) into (53) yields (43). ■

C. Proof of Lemma 3

Proof: Consider the candidate Lyapunov function $V_0 : \mathbb{R}^m \to \mathbb{R}_{\geq 0}$ defined as

$$V_0\left(e_0(t)\right) \triangleq \frac{1}{2}e_0^T(t)e_0(t). \tag{59}$$

Substituting (1) and (51) into the time-derivative of (50) yields

$$\dot{e}_0(t) = -k_0 e_0(t). \tag{60}$$

Substituting (60) into the time-derivative of (59) yields

$$\dot{V}_0\left(e_0(t)\right) = -k_0 e_0^T(t)e_0(t), \tag{61}$$

where substituting (59) into (61) yields

$$\dot{V}_0\left(e_0(t)\right) = -2k_0 V_0\left(e_0(t)\right). \tag{62}$$

Solving (62) yields $V_0(e_0(t)) = V_0(e_0(0))e^{-2k_0 t}$. Since $V_0(e_0(t))$ is radially unbounded with an unrestricted domain, equation (50) is globally exponentially regulated. Since $V_0(e_0(t))$ is positive definite and $\dot{V}_0(e_0(t))$ is negative definite, provided $k_0 > 0$, $V_0(e_0(t)) \in \mathcal{L}_\infty$. Since $V_0(e_0(t)) \in \mathcal{L}_\infty, e_0(t) \in \mathcal{L}_\infty$. Since $x_d(t) \in \mathcal{L}_\infty, x_0(t) \in \mathcal{L}_\infty$. Since $x_d(t) \in \mathcal{L}_\infty, \dot{x}_d(t) \in \mathcal{L}_\infty$, and $x_0(t) \in \mathcal{L}_\infty$, we see that $u_0(t) \in \mathcal{L}_\infty$. ■

Acknowledgment

Any opinions, findings, and conclusions or recommendations expressed in this article are those of the author(s) and do not necessarily reflect the views of sponsoring agencies.

References

[1] R. Olfati-Saber, J. A. Fax, and R. M. Murray, "Consensus problems in networks of agents with switching topology and time-delays," *IEEE Trans. Autom. Control*, vol. 49, no. 9, pp. 1520–1533, Sep. 2004.
[2] C. Mohan, "Blockchains and databases: A new era in distributed computing," *Proc. Int. Conf. Data Eng.*, 2018, pp. 1739–1740.
[3] N. Abaid and M. Porfiri, "Leader-follower consensus over numerosity-constrained random networks," *Automatica*, vol. 48, no. 8, pp. 1845–1851, 2012.
[4] L. Ding, Q.-L. Han, and G. Guo, "Network-based leader-following consensus for distributed multi-agent systems," *Automatica*, vol. 49, no. 7, pp. 2281–2286, 2013.
[5] X.-H. Wang and H.-B. Ji, "Leader-follower consensus for a class of nonlinear multi-agent systems," *Int. J. Control, Automat. Syst.*, vol. 10, pp. 27–35, 2012.
[6] J. Hu and G. Feng, "Distributed tracking control of leader-follower multi-agent systems under noisy measurement," *Automatica*, vol. 46, no. 8, pp. 1382–1387, 2010.
[7] W. Ren and R. Beard, "Consensus seeking in multiagent systems under dynamically changing interaction topologies," *IEEE Trans. Autom. Control*, vol. 50, no. 5, pp. 655–661, May 2005.
[8] Z. Kan, J. Shea, and W. E. Dixon, "Leader-follower containment control over directed random graphs," *Automatica*, vol. 66, pp. 56–62, 2016.
[9] M. Mesbahi and M. Egerstedt, *Graph Theoretic Methods in Multiagent Networks*. Princeton, NJ, USA: Princeton Univ. Press, 2010.
[10] A. Adaldo *et al.*, "Event-triggered pinning control of switching networks," *IEEE Trans. Control Netw. Syst.*, vol. 2, no. 2, pp. 204–213, Jun. 2015.
[11] D. V. Dimarogonas, E. Frazzoli, and K. H. Johansson, "Distributed event-triggered control for multi-agent systems," *IEEE Trans. Autom. Control*, vol. 57, no. 5, pp. 1291–1297, May 2012.
[12] T. H. Cheng, Z. Kan, J. R. Klotz, J. M. Shea, and W. E. Dixon, "Event-triggered control of multi-agent systems for fixed and time-varying network topologies," *IEEE Trans. Autom. Control*, vol. 62, no. 10, pp. 5365–5371, Oct. 2017.
[13] A. Adaldo, D. Liuzza, D. V. Dimarogonas, and K. H. Johansson, "Control of multi-agent systems with event-triggered cloud access," in *Proc. Eur. Control Conf.*, 2015, pp. 954–961.
[14] X. Dong and G. Hu, "Time-varying formation control for general linear multi-agent systems with switching directed topologies," *Automatica*, vol. 73, pp. 47–55, 2016.
[15] G. Wen, W. Yu, G. Hu, J. Cao, and X. Yu, "Pinning synchronization of directed networks with switching topologies: A multiple lyapunov functions approach," *IEEE Trans. Neural Netw. Learn. Syst.*, vol. 26, no. 12, pp. 3239–3250, Dec. 2015.
[16] C. Nowzari and J. Cortés, "Distributed event-triggered coordination for average consensus on weight-balanced digraphs," *Automatica*, vol. 68, pp. 237–244, 2016.
[17] P. Tabuada, "Event-triggered real-time scheduling of stabilizing control tasks," *IEEE Trans. Autom. Control*, vol. 52, no. 9, pp. 1680–1685, Sep. 2007.
[18] A. Adaldo, D. Liuzza, D. V. Dimarogonas, and K. H. Johansson, "Cloud-supported formation control of second-order multi-agent systems," *IEEE Trans. Control Netw. Syst*., vol. 5, no. 4, pp. 1563–1574, Dec. 2018.
[19] W. Heemels, K. Johansson, and P. Tabuada, "An introduction to event-triggered and self-triggered control," in *Proc. IEEE Conf. Decis. Control*, Dec. 2012, pp. 3270–3285.
[20] X. Yi, K. Liu, D. V. Dimarogonas, and K. H. Johansson, "Dynamic event-triggered and self-triggered control for multi-agent systems," *IEEE Trans. Autom. Control*, vol. 64, no. 8, pp. 3300–3307, Aug. 2019.
[21] Y. Fan, L. Liu, G. Feng, and Y. Wang, "Self-triggered consensus for multi-agent systems with zeno-free triggers," *IEEE Trans. Autom. Control*, vol. 60, no. 10, pp. 2779–2784, Oct. 2015.
[22] Z. Feng and G. Hu, "Secure cooperative event-triggered control of linear multiagent systems under DoS attacks," *IEEE Trans. Control Syst. Techol.*, vol. 28, no. 3, pp. 741–752, May 2020.
[23] N. H. Vaidya, L. Tseng, and G. Liang, "Iterative approximate Byzantine consensus in arbitrary directed graphs," *Proc. ACM Symp. Prin. Distrib. Comput.*, 2012, pp. 365–374.
[24] J. Hromkovič, R. Klasing, A. Pelc, P. Ruzicka, and W. Unger, *Dissemination of Information in Communication Networks: Broadcasting, Gossiping, Leader Election, and Fault-Tolerance*. Berlin, Germany: Springer, 2005.
[25] H. J. LeBlanc, H. Zhang, X. Koutsoukos, and S. Sundaram, "Resilient asymptotic consensus in robust networks," *IEEE J. Sel. Areas Commun.*, vol. 31, no. 4, pp. 766–781, Apr. 2013.
[26] S. M. Dibaji and H. Ishii, "Resilient consensus of second-order agent networks: Asynchronous update rules with delays," *Automatica*, vol. 81, pp. 123–132, 2017.
[27] D. Senejohnny, S. Sundaram, C. De Persis, and P. Tesi, "Resilience against misbehaving nodes in self-triggered coordination networks," in *Proc. IEEE Conf. Decis. Control*, 2018, pp. 2848–2853.
[28] J. Usevitch and D. Panagou, "Resilient leader-follower consensus to arbitrary reference values," in *Proc. Annu. Amer. Control Conf.*, 2018, pp. 1292–1298.
[29] Y. Hou, J. Li, and Y. Pan, "On the Laplacian eigenvalues of signed graphs," *Linear Multilinear Algebra*, vol. 51, no. 1, pp. 21–30, 2003.
[30] T. Zaslavsky, "Signed graphs," *Discrete Appl. Math.*, vol. 4, no. 1, pp. 47–74, 1982.
[31] C. Altafini, "Consensus problems on networks with antagonistic interactions," *IEEE Trans. Autom. Control*, vol. 58, no. 4, pp. 935–946, Apr. 2013.
[32] M. E. Valcher and P. Misra, "On the consensus and bipartite consensus in high-order multi-agent dynamical systems with antagonistic interactions," *Syst. Control Lett.*, vol. 66, pp. 94–103, 2014.
[33] J. Qin, W. Fu, W. X. Zheng, and H. Gao, "On the bipartite consensus for generic linear multiagent systems with input saturation," *IEEE Trans. Cybern.*, vol. 47, no. 8, pp. 1948–1958, Aug. 2017.
[34] F. M. Zegers, P. Deptula, J. M. Shea, and W. E. Dixon, "Event-triggered approximate leader-follower consensus with resilience to Byzantine adversaries," in *Proc. IEEE Conf. Decis. Control*, Nice, France, Dec. 2019, pp. 6412–6417.
[35] Z. Kan, A. Dani, J. M. Shea, and W. E. Dixon, "Network connectivity preserving formation stabilization and obstacle avoidance via a decentralized controller," *IEEE Trans. Autom. Control*, vol. 57, no. 7, pp. 1827–1832, Jul. 2012.
[36] F. Pasqualetti, A. Bicchi, and F. Bullo, "Consensus computation in unreliable networks: A system theoretic approach," *IEEE Trans. Autom. Control*, vol. 57, no. 1, pp. 90–104, Jan. 2012.
[37] F. Pasqualetti, F. Dörfler, and F. Bullo, "Attack detection and identification in cyber-physical systems," *IEEE Trans. Autom. Control*, vol. 58, no. 11, pp. 2715–2729, Nov. 2013.

[38] A. Barboni, H. Rezaee, F. Boem, and T. Parisini, "Detection of covert cyber-attacks in interconnected systems: A distributed model-based approach," *IEEE Trans. Autom. Control*, vol. 65, no. 9, pp. 3728–3741, Sep. 2020.

[39] A. Rahnama and P. J. Antsaklis, "Learning-based event-triggered control for synchronization of passive multi-agent systems under attack," *IEEE Trans. Autom. Control*, vol. 65, no. 10, pp. 4170–4185, Oct. 2020.

[40] H. Liu, M. Xu, Y. Wu, N. Zheng, Y. Chen, and M. Z. A. Bhuiyan, "Resilient bipartite consensus for multi-agent networks with antagonistic interactions," *in Proc. IEEE 17th Int. Conf. Trust Secur. Privacy Comp. Commun/12th IEEE Int. Conf. Big Data Sci. Eng.*, 2018, pp. 1262–1269.

[41] E. Garoudja, F. Harrou, Y. Sun, K. Kara, A. Chouder, and S. Silvestre, "Statistical fault detection in photovoltaic systems," *Sol. Energy*, vol. 150, pp. 485–499, 2017.

[42] L. Li, H. Luo, S. X. Ding, Y. Yang, and K. Peng, "Performance-based fault detection and fault-tolerant control for automatic control systems," *Automatica*, vol. 99, pp. 308–316, 2019.

[43] J. R. Klotz, A. Parikh, T.-H. Cheng, and W. E. Dixon, "Decentralized synchronization of uncertain nonlinear systems with a reputation algorithm," *IEEE Trans. Control Netw. Syst.*, vol. 5, no. 1, pp. 434–445, Mar. 2018.

[44] E. Garcia, Y. Cao, and D. W. Casbeer, "Decentralized event-triggered consensus with general linear dynamics," *Automatica*, vol. 50, no. 10, pp. 2633–2640, 2014.

[45] B. E. Paden and S. S. Sastry, "A calculus for computing Filippov's differential inclusion with application to the variable structure control of robot manipulators," *IEEE Trans. Circuits Syst.*, vol. CS-34, no. 1, pp. 73–82, Jan. 1987.

[46] D. Shevitz and B. Paden, "Lyapunov stability theory of nonsmooth systems," *IEEE Trans. Autom. Control*, vol. 39 no. 9, pp. 1910–1914, Sep. 1994.

[47] V. I. Bogachev, *Measure Theory*. Berlin, Germany: Springer, 2007, vol. 1.

[48] H. K. Khalil, *Nonlinear Systems*, *3rd ed*. Upper Saddle River, NJ, USA: Prentice Hall, 2002.

[49] M. Mazo and P. Tabuada, "On event-triggered and self-triggered control over sensor/actuator networks," in *Proc. IEEE Conf. Decis. Control*, 2008, pp. 435–440.

[50] R. A. Horn and C. R. Johnson, *Matrix Analysis*. Cambridge, U.K.: Cambridge Univ. Press, 1990.

Federico M. Zegers received the B.S. degree in mechanical engineering, the B.S. degree in mathematics, and the M.S. degree in mechanical engineering from the University of Florida, Gainesville, FL, USA, in 2016, 2016, and 2019, respectively, where he is currently working toward the Ph.D. degree under the supervision of Dr. Warren Dixon.

His research interests include Lyapunov-based nonlinear and adaptive control, multi-agent systems, switched/hybrid systems theory, and robotics.

Patryk Deptula received the B.Sc. degree in mechanical engineering (major) and mathematics (minor) from Central Connecticut State University, New Britain, CT, USA, in 2014, and the M.S. and Ph.D. degrees in mechanical engineering from the University of Florida, Gainesville, FL, USA, in 2017 and 2019, respectively.

His current research interests include, but are not limited to, learning-based and adaptive methods, estimation and control, sensor fusion, multi-agent systems, human–machine interaction, vision-based navigation and control, biomedical systems, biomechanics, and robotics applied to a variety of fields.

John M. Shea received the B.S. degree in computer engineering, and the M.S. and Ph.D. degrees in electrical engineering from Clemson University, Clemson, SC, USA, in 1993, 1995, and 1998, respectively.

In 1999, he joined the Faculty of the Department of Electrical and Computer Engineering with the University of Florida, Gainesville, FL, USA, where he was promoted to Professor, in 2015. His research interests include wireless and military communications and networked autonomous systems.

Dr. Shea was the recipiet of the Technical Achievement Award for contributions to military communications from the IEEE Military Communications Conference (MILCOM), in 2012, the Ellersick Award from the IEEE Communications Society for the Best Paper in the Unclassified Program of MILCOM, in 2013 and 1996. He was the recipient of the Outstanding Young Alumni Award from the Clemson University College of Engineering and Science, in 2011. He was selected as a Finalist for the 2004 Eta Kappa Nu Outstanding Young Electrical Engineer. He has been an Editor for *IEEE Wireless Communications Magazine*, since 2010. He was an Editor for the IEEE TRANSACTIONS ON WIRELESS COMMUNICATIONS, from 2008 to 2012 and was an Associate Editor for the IEEE TRANSACTIONS ON VEHICULAR TECHNOLOGY, from 2002 to 2007. He was the Technical Program Chair for the Unclassified Program of MILCOM, in 2010.

Warren E. Dixon (IEEE, Fellow) received the Ph.D. degree from Clemson University, Clemson, SC, USA, in 2000.

He worked as a Research Staff Member and Eugene P. Wigner Fellow with Oak Ridge National Laboratory (ORNL), Oak Ridge, TN, USA, until 2004, when he joined the Mechanical and Aerospace Engineering Department, with the University of Florida, Gainesville, FL, USA, where he is an Ebaugh Professor and Department Chair. His research interests include the development and application of Lyapunov-based control techniques for uncertain nonlinear systems.

Dr. Dixon is an ASME and IEEE Fellow. He was the recipient of the 2015 and 2009 American Automatic Control Council (AACC) O. Hugo Schuck (Best Paper) Award, the 2013 Fred Ellersick Award for Best Overall MILCOM Paper, the 2011 American Society of Mechanical Engineers (ASME) Dynamics Systems and Control Division Outstanding Young Investigator Award, and the 2006 IEEE Robotics and Automation Society (RAS) Early Academic Career Award. He was the recipient of the Air Force Commander's Public Service Award (2016) for his contributions to the U.S. Air Force Science Advisory Board. He was/is an Associate Editor for *ASME Journal of Dynamic Systems, Measurement and Control*, *Automatica*, IEEE CONTROL SYSTEMS, IEEE TRANSACTIONS ON SYSTEMS MAN AND CYBERNETICS: PART B CYBERNETICS, and the *International Journal of Robust and Nonlinear Control*.